

Functional Dyes in Polymeric 3D Printing: Applications and Perspectives

*Original*

Functional Dyes in Polymeric 3D Printing: Applications and Perspectives / Gastaldi, M., Cardano, F., Zanetti, M., Viscardi, G., Barolo, C., Bordiga, S., Magdassi, S., Fin, A., Roppolo, I.. - In: ACS MATERIALS LETTERS. - ISSN 2639-4979. - 3:1(2021), pp. 1-17. [10.1021/acsmaterialslett.0c00455]

*Availability:*

This version is available at: 11583/2977036 since: 2023-03-15T14:21:37Z

*Publisher:*

American Chemical Society

*Published*

DOI:10.1021/acsmaterialslett.0c00455

*Terms of use:*

This article is made available under terms and conditions as specified in the corresponding bibliographic description in the repository

*Publisher copyright*

(Article begins on next page)

# Functional Dyes in Polymeric 3D Printing: Applications and Perspectives

Matteo Gastaldi, Francesca Cardano, Marco Zanetti, Guido Viscardi, Claudia Barolo, Silvia Bordiga, Shlomo Magdassi, Andrea Fin,\* and Ignazio Roppolo\*

Cite This: *ACS Materials Lett.* 2021, 3, 1–17

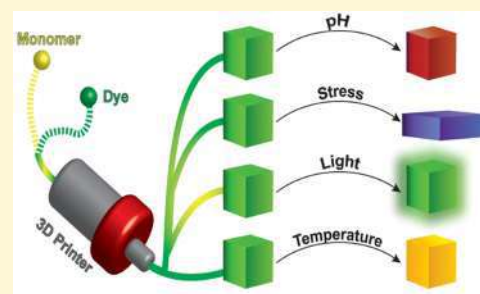
Read Online

ACCESS |

Metrics & More

Article Recommendations

**ABSTRACT:** Three-dimensional printing (3DP) is considered among the key-technologies for the next industrial revolution, with considerable effects on production processes, economy, and society. In this context, the most relevant part of the market consists of polymeric 3D printing. The 3D printable liquids are composed of various components, among them dyes are usually underrated because they are introduced merely for aesthetical reasons or to enhance the objects' resolution. In recent years, the capability of specific dyes to go beyond conventional use and to confer functional properties to 3D printed objects has become an emerging research area. Modifying elastic moduli upon light irradiation, inducing optical and emitting properties in the matrices or conferring temperature responsivity are just few examples of innovative stimuli-responsive materials that can be produced by combining well-designed dyes with the appropriate 3DP printed matrices. In this Review, we discuss and critically analyze the most relevant recent results achieved in the use of smart dyes in the synthesis of stimuli responsive 3D printed polymers.



Humans learned thousands of years ago how to modify the color of the materials by adding dyes and pigments for aesthetical purposes, as well as for peculiar functions (e.g., camouflage, heat dissipation). Over the centuries, this knowledge has been adapted to various classes of materials, including paintings, ceramics, and textiles. Polymeric materials underwent similar processes since the 19th century and different approaches were developed for dispersing organic dyes and pigments in polymeric matrices.

Conferring new functionalities to polymeric materials using dyes is particularly advantageous since a small amount of dye could remarkably change the properties of the material, while retaining the mechanical features of the matrix.

Recently, the use of small organic chromophores in polymers has found new scope, mainly addressed to transfer a plethora of features into the polymer libraries beyond the chromic tone. The preparation of materials capable to modulate color, mechanical, chemical, and optical properties under external stimuli are only few examples of these appealing

functional polymers.<sup>1–5</sup> Coumarins, azodyes, metal–organic complexes, spiropyrans, and naphthalene diimides are some examples of the functional dye employed in these applications.<sup>6–10</sup> Conferring new functionalities to polymeric materials using dyes is particularly advantageous since a little amount of dyes could remarkably change the properties of the material while retaining the mechanical features of the matrix. Moreover, the possibility to variously decorate the chemical structures of the dyes allows insertion in the polymeric matrices either by dispersion or by covalently link them to the polymeric backbones.

In recent years, functional dyes have found a key-role also in the field of 3DP. Recent improvements and innovations have encouraged the scientific and industrial research to enlarge the palette of available printable materials, towards new applications.<sup>11,12</sup> The first and more important use of dyes in 3DP is for aesthetical purposes, and even today the main request of the market is related to the color/transparency of a component.<sup>13,14</sup> Additionally, in some 3DP technologies, the

Received: September 24, 2020

Accepted: November 17, 2020

Published: November 25, 2020



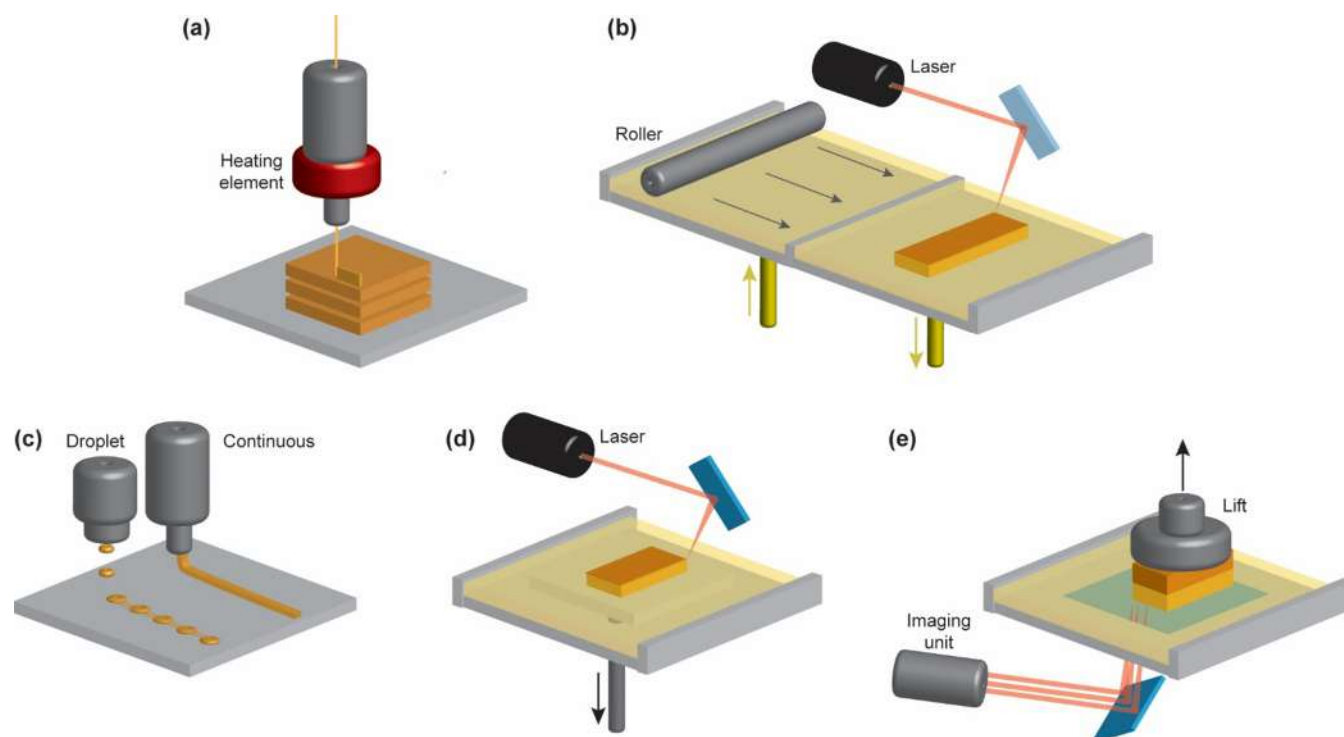


Figure 1. Graphical representation of printers in (a) FFF, (b) SLS, (c) DIW, (d) SLA, and (e) DLP.

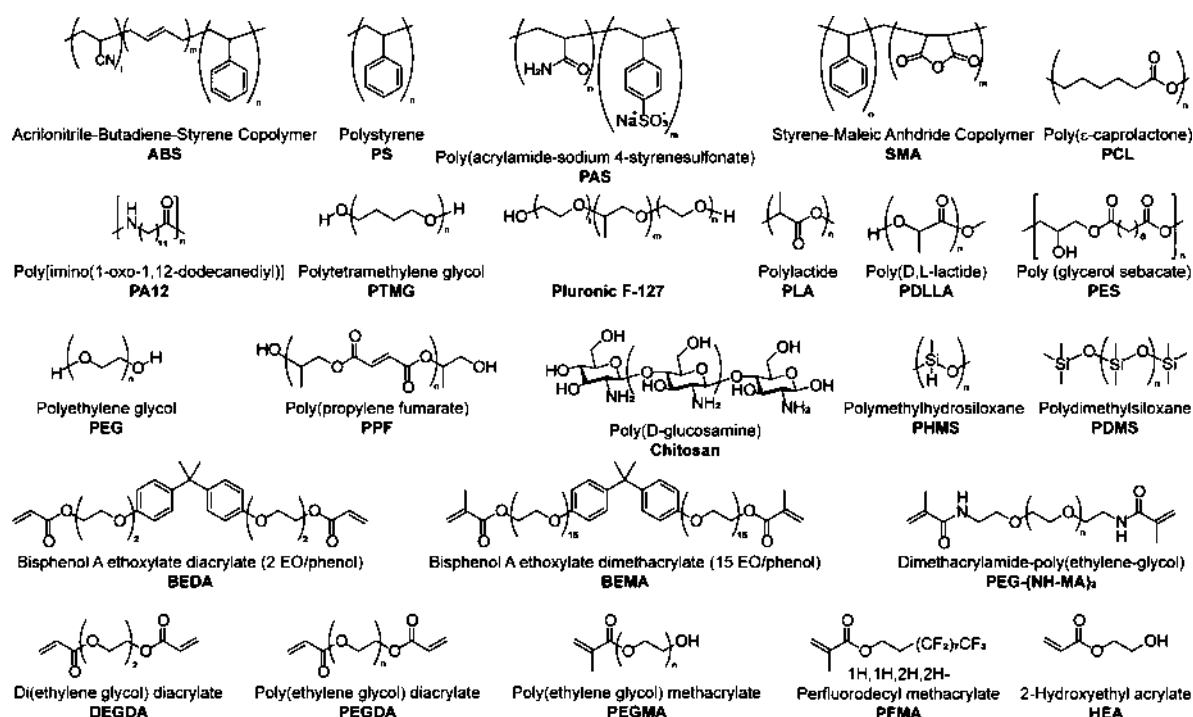


Figure 2. Chemical structure of commercially available polymers and monomer for application in 3DP.

dyes' role is intrinsically fundamental, determining printability and resolution.<sup>15</sup> On the other hand, fine-tuned chromophores are gaining an additional interest because of the possibility to translate their properties in the final 3DP objects. This approach has led to a relatively unexplored research area, in which materials properties and 3D structuration are merged in new synergistic effects.

The scope of this Review is to critically analyze the recent advancements in the use of dyes in polymeric 3DP to create objects responsive to specific external stimuli such as light, pH, temperature, and solvents.

In the first part, the 3DP techniques are described with a specific focus on the role of the dyes in each technology. Later, innovative uses of dyes in each 3DP technique are discussed, highlighting the key role of those components.<sup>16–21</sup> Finally, a

critical analysis is reported, to highlight the achieved results and future perspectives.

### ■ THREE-DIMENSIONAL PRINTING

The history of 3DP has began in the 1980s, with the first patents of stereolithographic apparatus (SLA), fused filament fabrication (FFF), and selective laser sintering (SLS).<sup>22–24</sup> The common first stage in all the 3DP techniques resides on the design of a computer-aided design (CAD) file, a virtual model of the desired final product. The CAD file is then sectioned into 2D layers by dedicated software and sent to the printer, which will produce the part. 3DP allows the objects' construction by controlled adding of materials. Material saving, personalized production, on-demand fabrication, production of objects with architectures not achievable with other methods are some advantages among many of 3DP. Over the years, those technologies have increased their popularity due to the progressive printers' cost reduction, mainly by the cessation of many patents. In parallel, the development of the printers has led to increased printing speed and an improved resolution of the final objects, making these techniques attractive for many manufacturing fields.

Metals, ceramics, and biological materials can be 3D printed, but in this Review, we'll focus on polymeric 3D printing.<sup>25–29</sup> Polymers play a leading role in 3DP market thanks to the possibility to modulate the final properties according to the expected applications.<sup>30–36</sup> 3DP has been investigated to overcome the limitation of conventional polymers production processes, becoming nowadays a consolidated alternative solution.

The most common AM techniques are briefly described in the next paragraphs, with their related advantages and drawbacks. The description includes FFF, SLS, direct ink writing (DIW), SLA, digital light processing (DLP), and two-photon 3D printing (TPP) (Figure 1). Some of the most common materials employed in these techniques are also reported to facilitate the reading (Figure 2).

**Fused Filament Fabrication.** FFF is the most common and widely used 3DP technique (Figure 1a). It consists in a controlled deposition of melted or semi-melted polymers through a heated nozzle. An extruder is fed with a thin filament of thermoplastic polymer (usually of 1.75 or 3 mm), which deposits a layer of material according to the digital model.<sup>37</sup> At the end of a layer, the printing head lifts up on Z-direction of one step, which corresponds to the slicing of the CAD file, and starts to print a new layer on the previous one. The possibility to print large dimension objects, the high user-friendly and the plethora of printable polymers, make this technique the most commonly used in industry. The overall efficiency and quality of the printing process depends on many parameters that must be well-specified.<sup>38,39</sup>

Among the many commercially available or synthetic thermoplastic polymers, acrylonitrile–butadiene–styrene copolymers (ABS), polyamides (PA), polycarbonate (PC), and polylactide (PLA) are the most used.<sup>37</sup> Fillers, such as fibers or metallic particles, can be added to tune or confer specific properties to polymeric matrices in various applications.<sup>40,41</sup> Moreover, a further implementation resides in the usage of multiple printing nozzles, which enable the printing of multimaterial objects with different designs and structures.<sup>42</sup> FFF is a mature technology with few drawbacks, among which, the most important one is related to the limited resolution to about 50  $\mu\text{m}$ . This hampers the printing of complex geometries

(e.g., hanging parts) for which temporary supports, removed by chemical or mechanical treatments at the end, are needed during the printing process.

Dyes are not necessary components of FFF's filaments, they are typically used for aesthetical purposes without any other specific functionality. Those dyes need to possess sufficient thermal stability to not degrade during the melting/extrusion step of the filament. This strongly limits the use of organic dyes, especially in high performance polymers, which requires high extrusion temperatures. Nevertheless, recently chromophores were introduced in this 3DP technique to confer innovative features to the polymeric matrix, as described in the next paragraphs.

**Selective Laser Sintering.** In SLS, a high-power laser is used to sinter metals, glasses, ceramics or polymer powders. The laser scans the powder bed in XY directions to sinter the desired points, following the CAD project (Figure 1b). Once a layer is completed, the building stage lowers down by one thickness step and a new layer of powder is deposited and scanned by the laser. The process is repeated until the printed object is fabricated.<sup>43</sup> The most used polymers in SLS are polyamide 12 (PA12), polystyrene (PS), and polycarbonate (PC); nevertheless, the limited availability of materials is the main limitation in this technique.<sup>44,45</sup>

The SLS processing temperature must be precisely controlled to obtain an optimal adhesion between layers and good resolution. In semicrystalline polymers, the processing temperature must be fixed in between the melting and the crystallization values.<sup>44</sup> Other key-factors to take into account are the powder's capability to absorb the laser wavelength, the laser irradiation intensity, the melted material viscosity, and the shape and size of the powder, which should be preferentially spherical and in a range between 20 and 80  $\mu\text{m}$ .<sup>44</sup> Moreover, the chamber must be kept in inert atmosphere to prevent any oxidative process during printing. Differently from FFF, supports are not needed for hanging parts since the non-sintered powder acts as a support for top layers. Furthermore, unsintered materials are also recovered and reused in the following processes. This makes SLS a widely diffused technique for industrial applications, especially for structural components. Dyes in SLS suffers of the same limitations described in FFF, since high temperatures are required in the sintering step. To the best of our knowledge, there are yet no examples of dyes used to confer specific properties or functionalities to SLS printed objects.

**Direct Ink Writing.** The working principle of DIW is very similar to FFF with the only difference that this technique enables the printing of inks with high viscosity or eventually shear-thinning.<sup>32</sup> A syringe is fed under a pneumatical compression or a screw, extruding the material at a fine-controlled temperature, pressure, and viscosity (Figure 1c). This process allows the polymer to be deposited according to a CAD file on a building stage.<sup>46</sup>

DIW is widely used in printing biological materials, using various materials, such as polymers, ceramics, and composites are suitable for DIW.<sup>47–49</sup> Nevertheless, each material requires peculiar extrusion speed to obtain a homogenous and well-defined final product.<sup>34,50–54</sup> Being an extrusion-based technique, the use of dyes is not strictly necessary in DIW, since they do not affect the printing process. However, recent examples reports on the use of chromophores in photoluminescent, pH, or thermoresponsive DIW printed materials containing various organic dyes.

**Photopolymerization Techniques.** In 1986, Charles Hull patented the first 3D printer based on photopolymerization.<sup>22</sup> Photopolymerization is a well-known polymerization process induced by light irradiation, presenting several intriguing advantages (e.g., high rate and stereospecificity), which made it appealing for applications in coating industries and electronic and inks technology.

The photopolymerization process takes place upon irradiation with light in the ultraviolet, visible, or near-infrared region of the spectra.<sup>55–59</sup> Photoinitiators absorb radiation and generate reactive species (e.g., radicals or cations) that react with the functional moieties present on the monomers, that propagate leading to the polymerization. The photocurable formulations, including 3D printable formulations, are usually liquid and are composed of several ingredients that will be introduced afterward according to 3D printing technologies.

SLA, DLP, and TPP are the three main techniques based on photopolymerization each one presenting advantages and drawbacks. The main difference in comparison to the above-discussed techniques resided on the fact that the photopolymerization-based techniques produce thermosets polymers (e.g., polymers with three dimensional crosslinked networks). Here, we'll use the term vat polymerization (VP) techniques for all the photo-induced 3D printing technologies.

**Stereolithographic Apparatus.** In the SLA approach/method, a reservoir (or vat) is filled with a photocurable formulation and a UV laser (e.g., 355 nm) scans the surface, according to a CAD project, inducing the photopolymerization process and curing the monomers (Figure 1d).<sup>55</sup> The XY plane resolution and the penetration depth along Z axis depend on many factors, including the instrumental parameters, such as the exposure time, the scan speed and the intensity of the light source, as well as chemical variables as the presence of additives and fillers.<sup>42</sup> When a layer is built, the building platform is lowered in the vat, new liquid resin covers the cured layers and another slice can be polymerized in the same way. Once the process is done, a post-curing stage in a UV oven is often needed to complete the polymerization and confer enhanced mechanical properties to the final object. SLA allows printing materials with different properties by varying the photocurable formulation of the operating liquid resins. On the other hand, because of the instrument configuration, multimaterial printing is not possible on XY plane, while it is possible to change materials along Z adjusting the photocurable formulation during the process. Furthermore, if compared with FFF, the printing rate is slower.

**Digital Light Processing.** DLP is an evolution of SLA, where a projector (e.g., emission wavelength at 405 nm) equipped with a digital mirror device (DMD) is located under the vat and projects the image of each cross-section into the liquid resin. The projection occurs through the transparent bottom of the vat and follows the CAD project (Figure 1e). DLP presents some advantages compared to SLA in terms of shorter production times because of the simultaneous polymerization of an entire layer, usage of a lower volume of resin per produced object, lack of restriction in height of the printed parts, minimal cleaning steps of the final products and high resolution (30–50  $\mu\text{m}$ ).<sup>42</sup> Similarly to SLA, a post-curing step with UV light is needed to complete the polymerization of all the reactive groups. Moreover, an LCD screen can be used instead of a DMD device to assemble 3D printers, saving costs but sacrificing the overall printing resolution.

As SLA evolution, DLP also suffers from similar drawbacks like the production of multimaterial objects, reduced printing dimension on XY plane, which makes this technology less appealing for some industrial applications, where huge printing section is necessary.<sup>42</sup>

**Two-Photon 3D Printing.** TPP offers the possibility to print objects with a resolution at the micrometer and nanometer scale. TPP is based on femtosecond pulsed laser, highly focused on a liquid resin, generating an high photon absorption probability on the focus area while keeping it very low outside.<sup>60</sup> As a result, a very tiny voxel is polymerized, allowing the fabrication of objects with high resolution, below 100 nm.<sup>61</sup> The low printing speed, the lack of efficient photoinitiators, and the reduced dimensions of the printed objects relegate TPP mainly to academic research, especially on biological, micromechanics, and optics fields.<sup>62</sup>

**3D Printable VP Formulations.** To explain better the importance of dyes in VP 3DP, here, we briefly describe the components of photocurable formulations. Those can be adapted to all the above-mentioned 3DP technologies based on photopolymerization, slightly modifying the ingredients. Each formulation is mainly composed of a monomer, a photoinitiator, and a dye.

Many monomers are commercially available, and in recent years, many other resins have been developed, reported, and reviewed.<sup>37,63</sup> The most common monomers in VP configuration are acrylates or methacrylates, with two or more polymerizable groups. Monomers with only one polymerizable group, such as acrylic or methacrylic acid, can also be used by adding a cross-linker. Unfortunately, these kinds of resins suffer from volume shrinkage during the polymerization process. Most of the acrylate systems can show strong internal stresses and deformations responsible for the reduced resolution or breakage of the final objects.<sup>55</sup> On the other hand, methacrylate monomers are less subject to shrinkage, but their curing rate is slower than acrylates.<sup>15</sup> A rapid curing process along with low final distortion of objects can be obtained by mixing acrylate and methacrylate monomers.<sup>37</sup> As an alternative, aromatic or high molecular weight (meth)acrylates, which present less volume shrinkage but higher viscosity, can be used.<sup>64,65</sup> Nevertheless, in these cases the printing parameters must be well-controlled and heating of the formulation during the printing process should also be considered.<sup>25</sup> Epoxy resins and thiol–ene systems (i.e., thiol monomers that react with alkene or alkynes) can also be used in VP as long as the monomers present at least two reactive groups to produce thermosets. These formulations show a reduced shrinkage, fewer stresses, and higher conversion in comparison to acrylate monomers.<sup>66,67</sup> For thiol–ene systems, the weakening of the mechanical properties due to the presence of –C–S–C– bonds can be reduced by the addition of allyl ethers to the thiol/methacrylate mixtures.<sup>68</sup> Finally, polymers with higher  $T_g$  can be obtained replacing alkene with alkyne in mixture with thiols monomers.<sup>69</sup> At last, it is worth mentioning that while the reactive groups of the monomers control the kinetics of the reaction, the backbone of the monomers has more influence on the physicochemical characteristics (e.g., strength, hydrophilicity, brittleness), so both the aspect should be taken into account while formulating a 3D printable material.

The first step in a photopolymerization process is the generation of reactive species. This step requires a photoinitiator, able to absorb the irradiation wavelength and

While the reactive groups of the monomers control the kinetics of the reaction, the backbone of the monomers has more influence on the physicochemical characteristics (e.g., strength, hydrophilicity, and brittleness), so both aspects should be taken into account while formulating a 3D printable material.

generate radicals or cationic species that can further react with monomers. The photoinitiator determines the polymerization rate, the conversion of the functional groups, the final resolution, and the threshold of polymerization.<sup>62,70</sup> The penetration of light into the resin and the curing depth are two important parameters that control the final resolution in VP and are both depending on the photoinitiator. The curing depth ( $C_p$ ) is defined as<sup>71</sup>

$$C_p = D_p \ln\left(\frac{E}{E_c}\right)$$

where  $E$  and  $E_c$  are the laser exposure on the resin surface and the critical exposure of the resin under a specific laser irradiation wavelength, respectively, and  $D_p$  is the penetration depth<sup>71</sup>

$$D_p = \frac{1}{2.3\epsilon[I]}$$

where  $[I]$  is the concentration of the photoinitiator and  $\epsilon$  is its molar extinction coefficient. It is possible to regulate the resolution of the product to obtain the desired properties of the final object by adjusting the quantity and type of the photoinitiator, the exposure time for each layer, as well as the energy of the light source. Other important parameters that can affect the  $C_p$  are the light density, the monomer reactivity, the temperature, and the exposure time.<sup>72</sup>

The photoinitiator can be radical or cationic species, according to the mechanism used to start the polymerization. Cationic photopolymerization, or eventually hybrid cationic and radical, is more suitable for SLA because a 355 nm UV laser is optimal to interact with those photoinitiators.<sup>55</sup> At 405 nm, the typical wavelength of DLP printers, there is a higher availability of radical photoinitiators, so that systems are preferred.<sup>55</sup> Among others, chalcones can be used as efficient free radical photoinitiators with a strong absorption at 405 nm. These molecules can start the photopolymerization of acrylate in a very efficient manner, showing different and suitable properties according to the substituted groups.<sup>73</sup>

At last, dyes are typically organic or organometallic molecules that can be inserted in a polymer either by dispersion or by covalent linkage to the chains through appropriate functional groups. The introduction of dyes in polymers allows obtaining light-emitting devices, electroluminescent polymers, temperature sensors, mechanochromic materials, or liquid crystals dispersed in polymers.<sup>74–79</sup>

In VP, dyes are added into the formulation to improve the features of the objects, such as resolution or strength, while dyes absorb in the UV or visible range, not affecting the polymerization process itself.<sup>37</sup>

Similarly, the cure depth is dependent on the light absorber concentration and its molar extinction coefficient. Dyes are able to spatially confine the polymerization process into the irradiated areas, according to the CAD file, while avoiding over-curing phenomena both in width and depth.<sup>72,80</sup> The amount of dyes loaded in 3DP matrices must be evaluated considering the broadness of the absorption spectrum and the dye molar extinction coefficient to minimize competitive photon absorption processes with other components like photo-initiators or photo-crosslinkers. An overall good resolution and fast polymerization are thus related to a well-evaluated balance between the dyes and the photoinitiator percentage in the matrix. In summary, in most of the applications, dyes do not seem to lend other important functionalities to the formulation other than conferring color to the final product.<sup>80</sup> This effect could be obtained using dyes in very low concentration as reported for solving the yellowing of the resin during the printing process by the addition of ultramarine dye (0.01% wt).<sup>81</sup>

As an example, Sudan I 1 (Figure 3) is a dye that has been widely used to limit the curing depth and obtain better  $z$ -

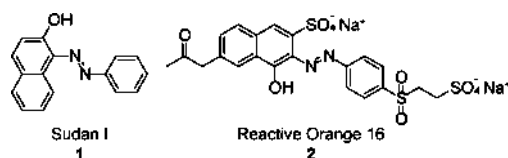


Figure 3. Structure of the UV-absorbing azodyes.

resolution.<sup>82,83</sup> For the same purpose, 1 was also mixed with diacrylate and thiol monomers showing a slower conversion reaction due to the competitive absorption among 1 and the photoinitiator.<sup>15</sup> This evidences that an optimal compromise should be carefully evaluated between curing rate and  $z$  resolution.

Similarly, Reactive Orange 16 2 (Figure 3) has been used to generate silver nanoparticle in situ using a formulation of PEGDA and  $\text{AgNO}_3$ .<sup>14</sup> The role of 2 was to avoid the curing out of the irradiated area and to control the thickness of each layer. Finally, 2 could also be degraded by UV light irradiation to obtain a decolorized final product.

The evolution in the use of dyes in 3DP is the goal of this Review, and it will be discussed in the following section, with particular focus on the synthesis of stimuli-responsive and functional polymers.<sup>84</sup>

As last ingredient of photocurable formulations, fillers can be added to synthesize (nano)composites and to impart some specific properties, such as electrical and thermal conductivity, luminescence, and tunable stiffness to the polymers. This is the most common strategy to overcome polymeric materials limitations. In this regard, 3D printing of composites is largely investigated and recently reviewed.<sup>41,85–88</sup>

## FUNCTIONAL DYES IN 3D PRINTING

Recent advances in using functional dyes in 3DP are discussed, while extensive reviews of chromophore molecules are reported elsewhere.<sup>89–97</sup> A brief description of the dyes used in 3DP is reported based on their molecular structure along with a summary table (Table 1) of all the dyes discussed in this review.

Azodyes are widely used in 3DP because of a modular straightforward synthesis and functionalization. The peculiarity

Table 1. Dyes Used in 3DP

dyes (entry)	3DP technique	refs
	azodyes	
1, 2, 26, 27, 34, 35, 56, 57, 58	SLA, DLP, DIW, TPP	15, 80, 83, 121, 128, 139, 140
	spiropyrans	
3, 4, 5, 24, 25	FFF, DIW	109, 120
	coumarines	
19, 28, 29, 30, 31, 44, 59, 60, 61, 62, 63, 64, 65, 66, 67, 68, 69, 70, 71	DIW, TPP	62, 115, 122, 125, 139, 141–143
	oligoaromatics	
6, 7, 8, 9, 10, 11, 12, 23, 33, 36, 37, 38, 39, 40, 41, 42, 43, 45, 49, 52	FFF, DIW, SLA, DLP	72, 85, 110–112, 117, 127, 130–133, 135, 138, 142
	metalloorganic complexes	
13, 14, 15, 16, 18, 20, 21, 22, 32	DIW	114–116, 126

of these dyes resides on capability to undergo reversible cis/trans isomerization upon UV or visible light absorption. The presence of various functional groups on the azo scaffold can confer unique photophysical features such a remarkable absorption shift between the cis and trans forms. Moreover they can be inserted in polymeric matrices as dispersed or covalently linked chromophores finding applications as photo-actuators, solar energy converters, and mechanical devices.<sup>90,98,99</sup>

Another family of stimuli-responsive dyes in 3DP, covering a broad range of absorption spectra, is based on spiropyranes. These compounds are usually classified as photoswitches, since they are able to isomerize to merocyanine form upon external stimuli, such as temperature, redox potential, solvents, metals, acids, or bases.<sup>96</sup> Applied mechanical forces can also induce the dye isomerization when they are inserted in polymeric matrices. Spiropyranes are characterized by absorption in the UV window, while the merocyanines show bathochromic shifted maxima in the 550–600 nm range of the spectra. These compounds are usually used in optical data recorders, as well as light filters and photochromic lenses.<sup>93</sup>

Coumarin derivatives are small aromatic dyes, composed of fused benzene and  $\alpha$ -pyrone rings, and characterized by high values of brightness and fluorescence quantum yield.<sup>100,101</sup> Because of their unique photophysical features and biocompatibility, coumarins have been widely used in 3DP, biomedical applications and organic light-emitting diodes devices.<sup>95,102</sup>

Other oligoaromatic dyes, spreading from condensed scaffolds like modified naphthalenes, functionalized rhodamine or rosin backbones, as well as extended  $\pi$ -systems like polymethine dyes or thiophene coupled with benzoxazoles, have been explored in 3DP application. Each specific scaffold is characterized by particular features. As a general statement, all the oligoaromatic dyes show good photo and thermal stability along with a high versatility.<sup>103–105</sup> In particular, polymethine dye present high values of molar extinction coefficient which makes them suitable for applications related to photodynamic therapy and dye-sensitized solar cells.<sup>106</sup>

Finally, metallo-organic complexes complete the library of dyes used in 3DP thanks to their high thermal and photostability while able to emit in the visible range. The high cost due to the presence of transition metals represents a limitation, but the low amount needed, usually less than 1% w/

w, and the remarkable features have prompted their use in 3DP, displays, and sensors devices.<sup>107</sup>

The dyes employed in each technology are introduced with a particular focus on the compromises needed to merge specific dyes and process peculiarities.

**Organic Molecules and Dyes in FFF.** Few functional dyes were employed in FFF 3DP because of the unfortunate possibility of thermal degradation during the extrusion.

Mechanochromic dyes are a class of chromophores known to change color when subjected to mechanical stress.<sup>78</sup> Aggregachromic dyes can be dispersed into the polymeric matrix and they are able to modify their optical properties when disaggregating after the exposure to a mechanical force or due to the mechanically induced chemical rearrangement of the chromophores covalently connected to the polymeric chains.<sup>78,108</sup> Mechanochromic spiropyranes in FFF have been recently introduced showing a color change from colorless to purple upon mechanical elongation due to the reversible switch between the spiropyran and merocyanine isomers (Figure 4a).<sup>109</sup> Three different spiropyranes 3–5 (Figure 4b) were

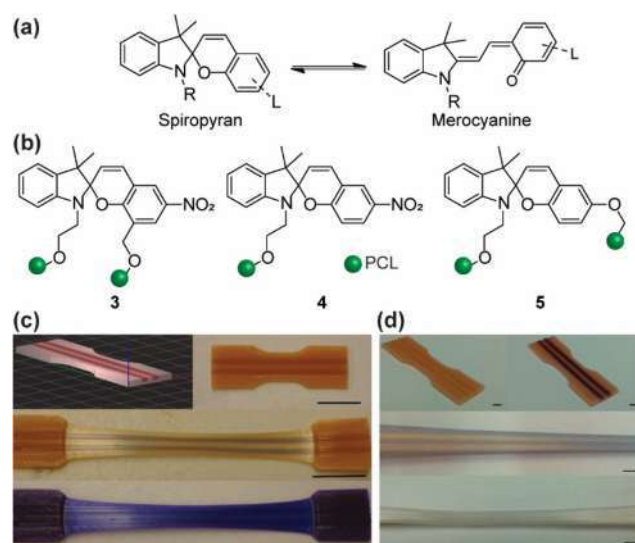


Figure 4. (a) Schematic representation of the reversible isomerization between spiropyran and merocyanine. (b) Spiropyran-containing polymer structures 3 and 4. (c) CAD representation, photos of the pre-elongated specimen, the post-elongated specimen before and upon irradiation at 365 nm of polymers containing 3 and 4. (d) Test specimen composed of 5 with stripes of 4 before and upon irradiation at 365 nm as well as under and after load. Adapted with permission from ref 109. Copyright 2015 American Chemical Society.

copolymerized via ring opening polymerization with PCL to obtain two matrices bearing the dyes inside the polymeric chain, in which the elongation stress was focused mainly on C-spiro-O bond, and one sample with a spiropyran as chain-end, in which the force cannot trigger the isomerization reaction. The polymers were printed by extrusion at 110 °C and without evidence of thermal degradation during the process, indicating the compatibility of these dye with FFF technology. Moreover, the purple color of the merocyanine form was not observed, suggesting that the stress during the printing process did not promote the chemical rearrangement of the dyes.

The reversible color changes were finally evaluated as a response to external mechanical stress or to UV irradiation,

suggesting potential applications in various devices. In particular, it could be possible to use these materials as sensor as well as to obtain immediate information about the tensile state of the structures (Figure 4c and 4d).

An inexpensive, biodegradable, and biocompatible colorful polymer printed in FFF was obtained by mixing a PLA matrix with crystals of a thermochromic triclinic polymorph of alkoxyphenyl N-substituted naphthalene diimides 6–11 (Figure 5a).<sup>110,111</sup> The first sample composed of PLA and 4

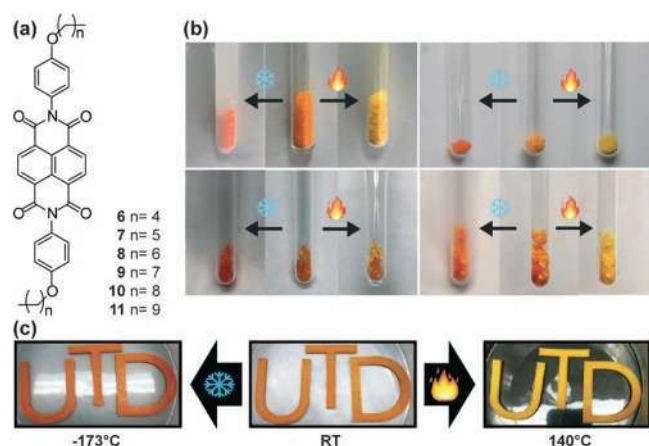


**Figure 5.** (a) Structure of NDI with various alkyl chains. (b) Thermochromic behavior of 7, 9, 10, and 11 at 100 and  $-173$  °C. (c) Reversible thermochromic behavior of composite between PLA and crystals of 6. Adapted from ref 110 with permission from The Royal Society of Chemistry.

(in 1:19 and 1:9 ratios) was melted at 200 °C without indication of thermal degradation and showing a reversible negative thermochromism, which was enhanced at higher concentration of 4. Similar but less evident positive thermochromism was obtained with 6 combined with PLA in a 1:9 ratio. The activation of the thermochromism at different temperature can be controlled by modulating the alkoxyphenyl chain length, making these materials suitable for thermal sensors. A clear change in color from deep orange to bright yellow can be obtained by exposing the 3DP object to very low ( $-173$  °C) or high (140 °C) temperatures (Figure 5b and 5c). This can be useful to produce structural parts that, at the same time, can act as temperature probes.

Photonic crystals are dielectrics materials in which an inner propagation of some light frequencies is forbidden providing a color proper of the crystal nanostructure. These materials can also be introduced in formulations as an alternative to dyes and pigments as in the case of the colorless dendritic block copolymer with a molecular weight of 484 kDa 12 (Figure 6a).<sup>112</sup>

During the FFF printing process at 200 °C, 12 rapidly self-assembles and produces a nanostructured material that can reflect violet and transmit yellow light (Figure 6b–d). The reflected light wavelength can be modulated within defined limits related to the processability, by increasing the molecular weight of 12. Not only violet, orange, and green light-reflected materials have been produced, but also a sample able to transmit light was obtained with further use as an optical filter.

FFF can be used to process colorful functional materials without occurring in degradation despite the temperature and mechanical stresses generated during the printing process. This

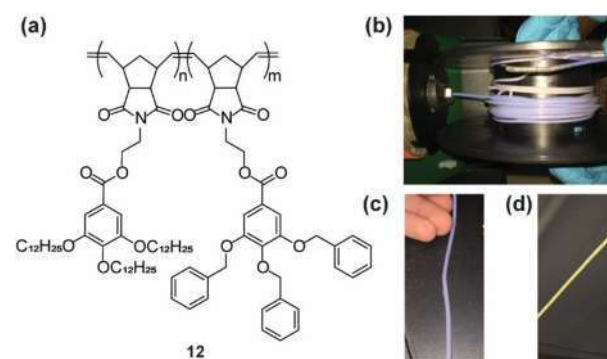


**Figure 6.** (a) Structure of the block copolymer 12. (b, c) Violet reflecting extruded filament. (d) Yellow transmitting extruder filament. Reprinted with permission from ref 112. Copyright 2017 American Chemical Society.

led to easy and low-cost production of functional materials with excellent resolution and complex geometries, making easy even-home production of components with high added value.

**Organic Molecules and Dyes in DIW.** DIW is a very good choice for the development of functional materials since it operates at room temperature while using liquids and pastes. One of the most important and exploited uses of DIW is to print hydrogels with cells that can mimic the extracellular matrix. Thanks to the low viscosity, hydrogels can be easily printed through an extrusion and the shape can be retained after the printing process by a rapid sol–gel transition or by a secondary cross-linking procedure that can be used to stabilize the final construct.<sup>113</sup> This technique is also known as bioprinting and was largely combined with the use of functional dyes.

A multifunctional 3DP hydrogel composed of sodium alginate, sodium polyacrylate and layered rare-earth hydroxide, consisting mainly of lanthanide ions of  $\text{Eu}^{3+}$  and  $\text{Tb}^{3+}$  13–16 (Figure 7a) was recently reported.<sup>114</sup> These ions, other than as co-cross-linkers, ionic carriers, and rheology modifiers could emit light and their photoluminescence could be tuned, by modulating the concentration of the cation in the hydrogel matrix composed of 17, sodium alginate, and sodium polyacrylate matrix (Figure 7b). The emission, under 254 nm UV light, shifted from yellow to red and green according to the different ratios between the  $\text{Eu}^{3+}$  and  $\text{Tb}^{3+}$ . These final properties, along with the high-resolution printability and the tunable stiffness has permitted the creation of skin like sensors capable to detect human motion.

Photoluminescent 3DP hydrogels were also used to evaluate the  $\text{O}_2$  concentration available for cells.<sup>115</sup> A  $\text{O}_2$ -sensitive luminescent platinum(II) meso(2,3,4,5,6-pentafluoro)phenyl porphyrin 18 and a coumarin derivative 19 as a fluorescence standard (Figure 7c) were dispersed in an alginate-based bio-ink with cytocompatible nanoparticles, made of styrene-maleic anhydride copolymer. The platinum complex has conferred a red emission upon excitation with blue wavelength, and it could change its emission as a function of  $\text{O}_2$  concentration. This probe was successfully used to map the oxygen concentration in printed objects containing green microalgae (*Chlorella sorokiniana*) and human mesenchymal stem (hTERT-MSC) cells (Figure 7d).

Similarly, transition metals ions were employed to print hydrogels by coassembling with the peptide hydrogelators.<sup>116</sup> The covalent bonds between the ligands, and the peptides

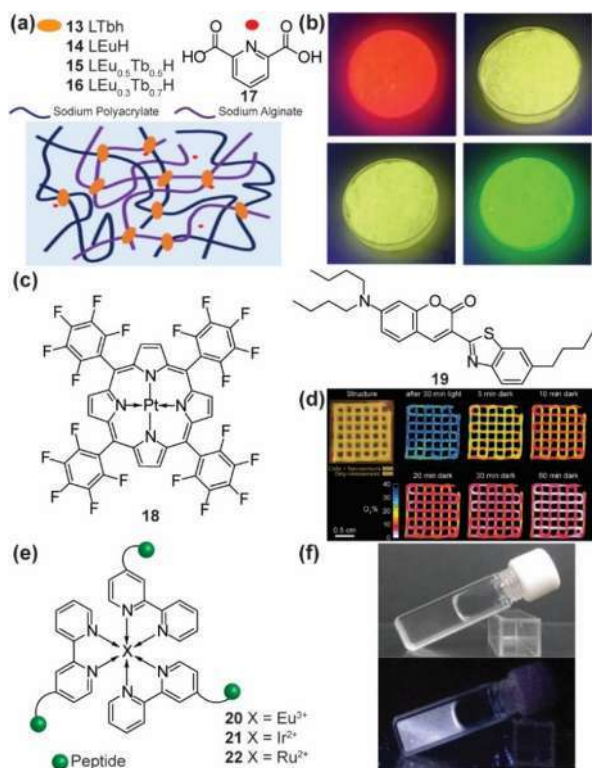


**Figure 7.** (a) Components and schematic representation of fluorescent hydrogels. (b) Emissive hydrogels containing 13–16 under 254 nm excitation. Reprinted with permission from ref 114. Copyright 2020 American Chemical Society. (c) Structures of the O<sub>2</sub> sensitive fluorescent Pt complex 18 and the coumarin derivative 19. (d) Spatiotemporal dynamics of O<sub>2</sub> concentration depicted by hydrogel containing 18, 19, and a layer of microalgae. Reprinted with permission from ref 115. Copyright John Wiley and Sons. (e) Structure of the bipyridine metal complexes 20–22 in hydrogel. (f) Natural and UV light illumination of hydrogel showing white emission. Reprinted from ref 116. Copyright Springer Nature.

were designed to prevent aggregation with consequent self-quenching of the chromophores. 2,2'-Dipyridine (bpy) as a ligand was used to realize the emitting complexes 20–22 with Eu<sup>3+</sup>, Ru<sup>2+</sup>, and Ir<sup>3+</sup> cations (Figure 7e). Different emission patterns, as well as a white fluorescent hydrogel, could be generated by playing with the relative ratios of the metals' complexes (Figure 7f). The final hydrogels were proven to be mechanically stable in water and suitable for application in soft electronics.

An interesting application of organic fluorescent dyes in the polymeric matrix demonstrated that not only the photo-physical properties but also the mechanical behavior of well-known and discussed hydrogels could be modulated by the presence of a chromophore (Figure 8a).<sup>46,117</sup> In a PAS matrix loaded with tetra-(4-pyridylphenyl)ethylene 23 (Figure 8b), pH variations were shown to induce (dis)aggregation phenomena of the dye which were depicted by a change in the monolayer emission (Figure 8c). At the same time, in an acidic environment, due to the increasing protonation of the dye and its consequent solubilization, the brightness decreased and a material deformation occurred, due to the electrostatic interaction between the protonated 23 and PAS. Both the dyes' concentration and the time needed to reach the equilibrium were investigated in detail.

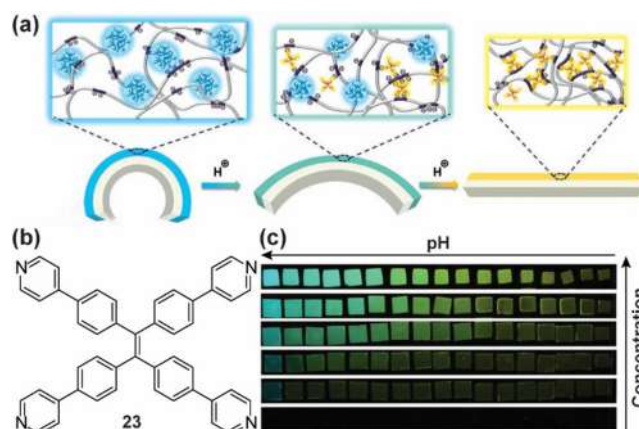


**Figure 8.** (a) Schematic representation of change in fluorescence and shape of PAS containing 23. (b) Molecular structure of 23. (c) PAS monolayer loaded with different concentration of 23 at different pH. Reprinted with permission from ref 117. Copyright John Wiley and Sons.

Another type of material able to change the shape through pH variation in a totally reversible and rapid way was designed by mixing PEG-(NH-MA)<sub>2</sub> with  $\alpha$ -cyclodextrin ( $\alpha$ -CD), creating a polypseudorotaxane 3DP hydrogel.<sup>118</sup> The material was not only responsive to pH variations because of the deprotonation of a hydroxyl groups of  $\alpha$ -CD, but, when mixed with polyacrylate, it was also sensitive to the variations in the aqueous ionic strength.

$\alpha$ -CD has also been reported in combination with Pluronic F-127 to create reversible shape 3DP hydrogel in response to solvent exchange between water and DMSO. It is worth noting how this effect could be used to convert solvent chemical energy into a mechanical one.<sup>119</sup>

The mentioned spiropyran can be also used in DIW in combination with commercial silicone inks composed of PDMS microbeads in which 24 was incorporated via platinum-catalyzed hydrosilylation in 0.25 wt % (Figure 9a).<sup>120</sup> The switch between spiropyran 24 and the merocyanine 25 was shown to be activated either by compression or elongation and to be completely reversible. The decoration of the 24 scaffold with a nitro group was translated in longer time needed to reverse the equilibrium from 25 in comparison to the unsubstituted dye (Figure 9b). The presence of the spiropyran moieties, conferring mechanochromic response, seems to have no effect on the pristine properties of PDMS microbeads.

Reversible deformation of printed polymers could also be achieved by using the *trans/cis* isomerization of azobenzene dyes 26 and 27 (Figure 9c).<sup>121</sup> PHMS with molecular weight of 2100–2400 g/mol were initially functionalized with 26 and 27 using platinum-catalyzed hydrosilylation reactions. The obtained material was subsequently printed via a syringe on a film of a commercial polyimide, which confers flexibility and excellent resistance against organic solvents. Under 442 nm irradiation, both materials have shown a deformation that could be totally recovered, in the second's time scale, once the light was switched off. After ten cycles the materials did not show fatigue (Figure 9d). Furthermore, relative contributions of Young's moduli and thicknesses of both layers could be used to modulate the motion of the materials.

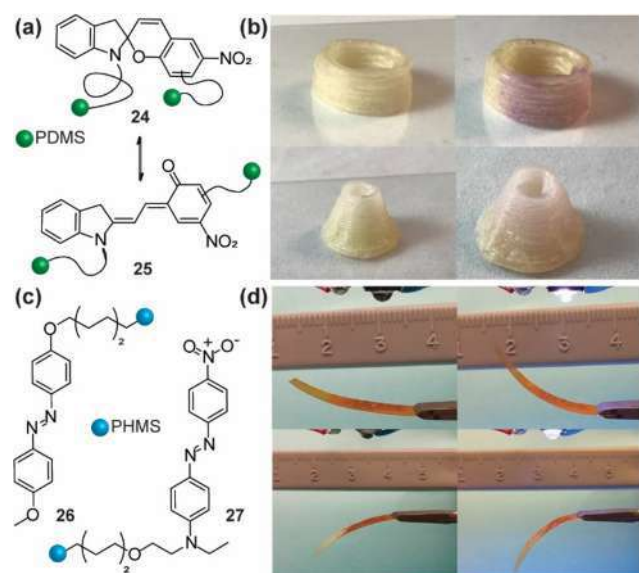


**Figure 9.** (a) Schematic representation of the reversible isomerization between spiroopyran 24 and merocyanine 25. (b) Images taken before and after application of force or compression showing a color change. Reprinted from ref 120 with permission from The Royal Society of Chemistry. (c) Structure of the azo dyes 26 and 27. (d) Images of polymer matrix containing 26 with UV LED off and on. Reprinted with permission from ref 121. Copyright 2018 American Chemical Society.

Coumarin can be used to reversibly modulate the mechanical properties of polymers by UV light irradiation to generate a polyester, derived from biorenewable resources.<sup>122</sup>

More in detail, soybean oil and adipic acid, readily available by extraction from biorenewable source, can be functionalized with coumarin derivatives, well-known fluorophores used in biomedical applications and characterized by low to none cytotoxicity.<sup>123,124</sup> Coumarin appendage 28 reacts via a [2 + 2] cycloaddition to form 29 under UV light (Figure 10a). Thanks to the reactivity of the coumarin, a 3DP and biodegradable polyester were prepared without the need of solvents and photoinitiators. The so obtained viscoelastic liquids change their properties to generate an elastomeric product by photo-cross-linking reaction upon irradiation at 350 nm (Figure 10b). This result highlighted the possibility to produce tunable bio-based polymers for biomedical purposes, with minimal toxicity of the initial components, while the usage of less intense light source should be considered to cure the hydrogel and to preserve the cell viability. The same approach was used to fabricate free-standing photo-cross-linked hydrogels exploiting the reversible [2 + 2] cycloaddition of coumarin 30.<sup>125</sup> Irradiation at 254 nm of the prepared hydrogel was depicted by complete reversible degradation into water-soluble copolymer 31, which have shown low acute cytotoxicity suggesting application as a cell-culture scaffold (Figure 10c).

A similar concept has been applied to ruthenium(II) tris-bipyridyl dication 32 and sodium ammonium persulfate to mediate the cross-linking of a 3D printed hyaluronic acid and gelatin hydrogels with phenolic hydroxyl moieties through visible light (Figure 10d).<sup>126</sup> The mechanical properties of the final polymer can be tuned varying the ruthenium concentration demonstrating the potential use in regenerative medicine.

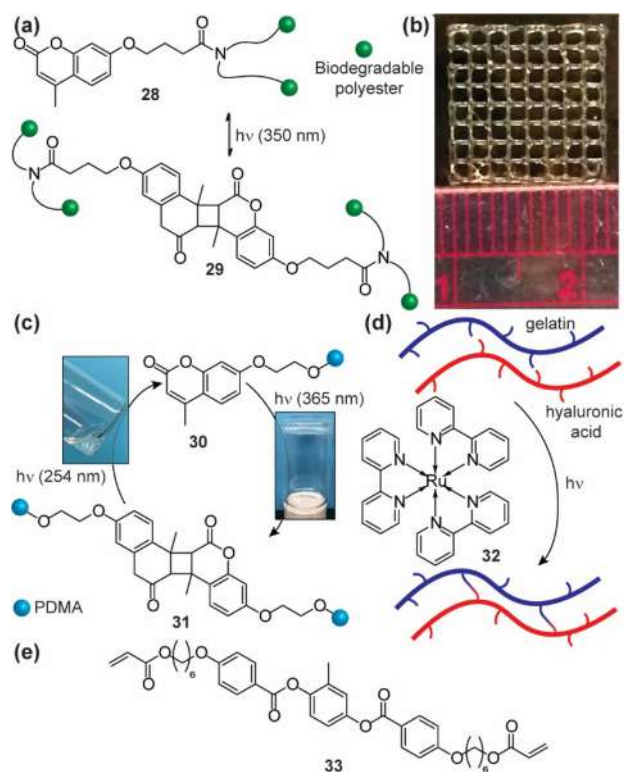


**Figure 10.** (a) Polyester photo-cross-linkage using 28. (b) 3DP bio renewable polyester containing 29. Reprinted with permission from ref 122. Copyright 2016 American Chemical Society. (c) Formation and recycling of the coumarin 30 cross-linked hydrogel by light. Reprinted with permission from ref 125. Copyright 2018 American Chemical Society. (d) Schematic representation of 32 and light mediated cross-linking between gelatin and hyaluronic acid. Adapted with permission from ref 126. Copyright John Wiley and Sons. (e) Molecular structure of liquid crystal elastomer 33.

Not only hydrogels can be printed in DIW but also liquid crystal elastomers (LCE), as reported for 33 (Figure 10e) when mixed with *n*-butylamine as a chain extender and a photoinitiator.<sup>127</sup> In the printing process, LCE were aligned along the printing pathway, and the material showed 40% of reversible contraction from room temperature up to 200 °C, only along the printing direction. The DIW printed structure was then photo cross-linked under UV light. These smart devices have been reported suitable for medical functions.

The reported examples show also that DIW can be a promising 3DP technique in which organic dyes can be successfully introduced in polymeric matrices. Light-emitting materials, reversible chemical reactions, or controlled shape deformations are the most promising properties conferred to objects obtained by merging dyes with DIW technique.

**Organic Molecules and Dyes in SLA/DLP.** SLA and DLP are the most suitable techniques for taking advantage of the use of the functional dyes since they work at room temperature and employing liquid formulations. Organic molecules and dyes can be introduced as additives in liquid formulations, conferring specific and useful functionalities or simply improving the control over the polymerization process and objects' final resolution. In the context of SLA and DLP techniques, the collection of the available dyes and polymeric matrices is wide and varied.

A variation on the Young's modulus have been reported by using well-known azodyes 34 and 35 (Figure 11a). Those were

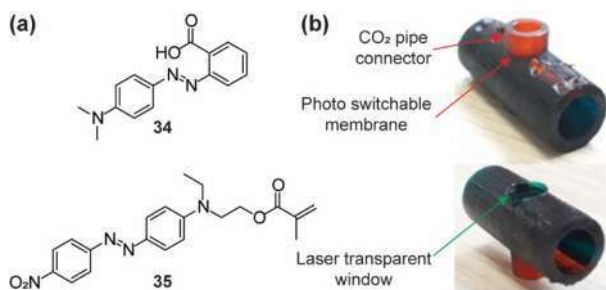


**Figure 11.** (a) Molecular structure of the azodyes 34 and 35. (b) 3DP prototype gas separator printed from a single CAD design. Reprinted with permission from ref 128. Copyright Elsevier.

used in two different polymeric matrices with similar chemical structures but different glass transition temperatures, namely BEDA with molecular weight of 572 g/mol and BEMA with molecular weight of 1700 g/mol.<sup>80</sup> Under laser irradiation at 532 nm, the Young's moduli of the two polymers showed remarkable changes depending on the polymers'  $T_g$  (BEMA has a  $T_g$  of  $-38$  °C, while BEDA  $46$  °C). BEMA with 35 increased its elastic modulus by 18% and BEMA with 34 by 58% at 25 °C. On the other hand, at the same temperature, BEDA reduced the elastic modulus by 27% containing 35, and with 34 by 75%. Furthermore, when the temperature was 48 °C, BEDA containing 34 increased Young's modulus by 620%, showing an opposite behavior. These experimental data were applied to microcantilevers to locally control changes in mechanical properties by laser irradiation.

The same azo dyes were employed in a following work to exploit the trans/cis switching of azobenzene dyes under visible light for 3D printed devices with photo-activated gas permeability.<sup>128</sup> The formulations were printed with DLP then CO<sub>2</sub> and O<sub>2</sub> permeability analyses were carried out on the resulting membranes under Nd:YAG laser beam irradiation at 532 nm and at different humidity conditions. Under laser irradiation, the CO<sub>2</sub> permeability was increased by 14% for PEGDA containing 35 and 70% for PEGDA doped with 34 at 25 °C and 0% of humidity. The processes were reported as completely reversible showing a carbon dioxide permeability increase when the laser was switched off. On the other hand, the CO<sub>2</sub> permeability was 30 times higher than O<sub>2</sub> permeability, and the laser irradiation seemed not to have an effect. Finally, a 3D prototype gas separator was printed from a single CAD file changing the printable formulation along z-axis and tested in CO<sub>2</sub> permeability. The device was built using the same polymeric in which alternatively a 532 nm transparent dye (brilliant green) and the azo-dye were used (Figure 11b). CO<sub>2</sub> was flowed through the azobenzene-based membrane and during laser irradiation, different CO<sub>2</sub> permeability was detected by monitoring the pH of the aqueous solution where the CO<sub>2</sub> gurgles, forming carbonic acid. The methacrylated azodye 35 was also used to obtain a defined 3DP microfluidic devices with microscale channels used to carry out precise biological analysis. The azodye improved the resolution both in z-direction, as well as in XY plane, avoiding the released of the chromophore during the use of the device.<sup>129</sup>

Environmentally sensitive materials, able to respond to variations in physical parameters, such as light and temperature, has been also reported using anthracene 36 in different polymeric matrices.<sup>130</sup> Anthracene can undergo [4 + 4] cycloaddition generating 37 under UV light with  $\lambda > 300$  nm

and the almost complete reversible reaction occurs under irradiation with  $\lambda < 300$  nm (Figure 12a). The printed



**Figure 12.** (a) Schematic representation of the photo cross-linking of 36. (b) Reprinted with permission from ref 130. Copyright Elsevier.

material, a linear 37-containing poly(D,L-lactide)-poly-(tetramethylene oxide) glycol copolymers (AN-PDLLAPT-MEG) with different content of PDLLA, showed recovery of the initial shape after deformation in the dynamic mechanical analysis (Figure 12b). Furthermore, the possibility to 3D print this material using SLA or DLP configurations without the need of a photoinitiator may ensure the biosafety and the possible use in biomedical applications. A 37-containing copolymers PLA and PEG exhibited dual stimuli responsivity to light and heat to deform and recover the initial shape. Moreover, the anthracene change in fluorescence before and after the irradiation at 365 nm could be exploited and used for information storage and simple anticounterfeiting.

Using DLP, it has been reported the preparation and 3DP of fluorescent resins able to emit in the three primary colors regions of the spectra, as well as to provide a white-emitting matrix when mixed.<sup>72</sup> Three different DEDGA-based formulations were prepared, containing different low molecular weight acrylates to enhance the solubility and dispersion of the photoinitiator as well as of the three dyes: BBO 38 for blue, Solvent Yellow 98 39 for the green, and Rhodamine B 40 for red resin (Figure 13a). The resulting clear resins were 3D printed and then studied in the cure depth, showing an excellent final resolution and the emission of white light with the possibility to fine-tune the emission mixing the three primary colors (Figure 13b).

Photoluminescent polymers can also be tuned for the preparation of high-tech materials like waveguides as recently reported for a BEDA matrix, along with a methacrylate benzoxadiazole 41, as smart dye in 0.01, 0.005, and 0.001 per hundred resin (phr) covalently linked to the polymer after the DLP process (Figure 13c).<sup>131</sup> The resins' printability, the intrinsic emission and the dependence on the dye concentration were investigated to show an inverse relationship between the material transmissivity and the dye concentration, probably because of the reabsorption processes (Figure 13d). Additionally, the printed device has shown potential application as a polarity sensor providing different emission upon interaction with various organic solvents.

Coordination polymers represent an alternative to conventional matrices to create interesting materials for chemosensing applications because of their high flexibility, dynamic

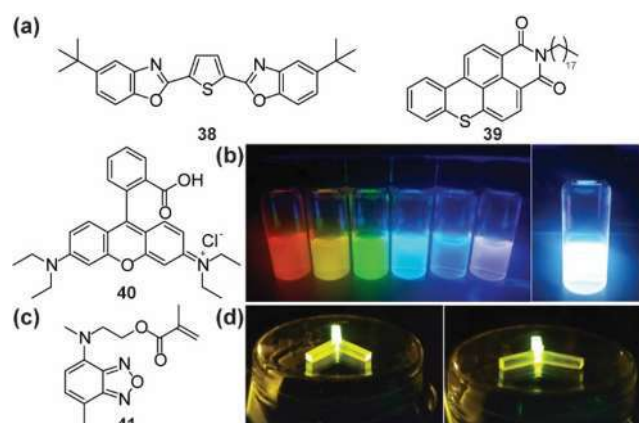


**Figure 13.** (a) Structures of three fluorophores 38, 39, and 40. (b) Emissive resins and white emission sample generated using 38–40 dyes. Reprinted with permission from ref 72. Copyright John Wiley and Sons. (c) Structure of benzoxadiazole 41. (d) Illuminated waveguides containing 41. Reprinted with permission from ref 131. Copyright 2018 American Chemical Society.

structures, and possibility to create stimuli-responsive devices. An example of such materials was introduced by employing the commercially available 4-4'-bipyridine 42 as metal coordinator in combination with copper(II) 1D coordination polymer inserted with thymine as a terminal ligand (Figure 14a and

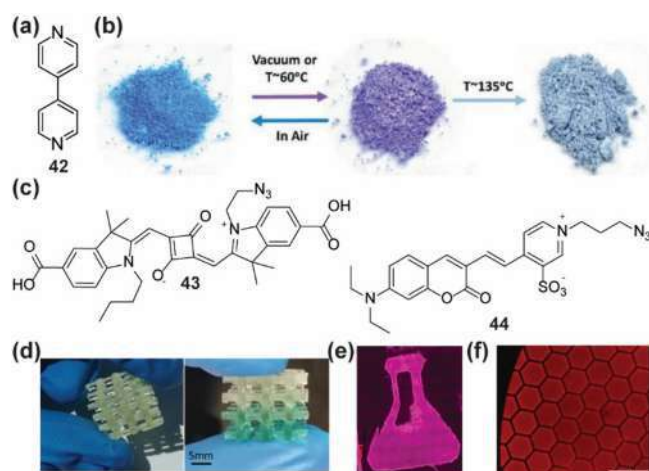


**Figure 14.** (a) Structure of the bipyridine ligand 42. (b) Polymer containing 42 color change over dehydration. Reprinted with permission from ref 85. Copyright John Wiley and Sons. (c) Structure of the azide dyes 43 and 44. (d) Hybrid structures printed object before and upon treatment with 43. Reprinted with permission from ref 132. Copyright The Royal Society of Chemistry (e) Printed fluorescent polyester stamp containing 44. Reprinted with permission from ref 133. Copyright 2018 American Chemical Society. (f) Microscopy image of PPF disc functionalized with 44. Reprinted with permission from ref 134. Copyright 2018 American Chemical Society.

b).<sup>85</sup> The polymer was characterized by both coordinated and solvation water molecules that were partially released by heating, causing a color shift from blue to violet. It is worth noting that the dehydration process was proven to be completely reversible, making this material suitable as a moisture sensor, also in organic solvents.

More complex dyes bearing reactive azide groups on a squaraine backbone as 43 was also used to react via click chemistry reaction with alkyne moieties showing high selectivity in a dedicated post-printing functionalization process (Figure 14c).<sup>132</sup> Two different formulations were prepared with the former containing an excess of reactive thiol, and the latter was characterized by an excess of alkyne moieties able to react with the 43 to provide selective staining on the printed object (Figure 14d).

The same copper-mediated azide–alkyne cycloaddition approach was used to functionalize complex polyesters with a modified coumarin 44 to confer emission properties to the polymer (Figure 14c).<sup>133</sup> The prepared copolymer, 3D printed with continuous DLP (cDLP), was further treated with 44 to quickly create a bright printed object (Figure 14e).

Due to that, these copolymers were employed for regenerative medicine, thanks to the biocompatibility and degradation into safe by-products. A clear example of such applications was recently reported 3DP with cDLP discs of PPF functionalized with propargyl alcohol moieties, which could further react with 44 by azide–alkyne click mechanism (Figure 14f).<sup>134</sup> The reactivity of the printed discs toward azides was visually confirmed by the color of the final objects. The same reaction was then applied to functionalize the PPF disc with N<sub>3</sub>-GRGDS peptide to prepare biocompatible scaffolds for application in biomedical treatments.

Mechanophores polymeric matrices represent an interesting alternative for the preparation of material responsive to external stimuli, as reported for HEA containing oxanorbornadiene 45 (0.99 wt %) and Irgacure 819 46 as photoinitiator (0.49 wt %).<sup>135</sup> The samples were prepared by DLP under visible light irradiation to avoid degradation of 45, while providing high efficiency of the crosslinking. Subsequent compression of the sample for one minute was shown to prompt the formation of the 47 and 48, which are the molecular constituents of 45 (Figure 15b). Furthermore, complex shape objects containing 0.01% wt Nile Red 49 were additionally printed to demonstrate the excellent final resolution and the possibility to reversibly compress these products (Figure 15c).

Natural or biocompatible materials were as well employed for VP polymerization. For instance, chitosan, a biocompatible and biodegradable polymer, is very attractive for biomedical applications. A bioink was obtained straightforwardly by functionalizing chitosan with methacrylic anhydride and finally mixed with LAP 50 (Figure 15c) to start the polymerization using 405 nm light source which is less harmful to cell lines compared to UV radiation.<sup>136</sup> The resulting polymer has shown high fidelity and resolution, along with biocompatibility.

PGS is another example of a biocompatible polymer that could undergo photo cross-linkage when mixed with an acrylate moiety 51.<sup>137</sup> The samples were characterized measuring the elastic modulus values as a function of the cross-linker concentration and the exposure time during the printing process. The final DLP printed samples have shown suitable mechanical properties and biocompatibility,

Those biomaterials were as well used with functional dyes as it has also been reported using a rosin derived monomer 52 and HEA in a mixture of methacrylated ethyl cellulose macromonomer 53 and hexamethylene diisocyanate 54 as cross-linkers.<sup>138</sup> The formulation was printed in SLA with 55 as photoinitiator and, subsequently, the thermoset was heated to promote a secondary cross-linking between 54 and free

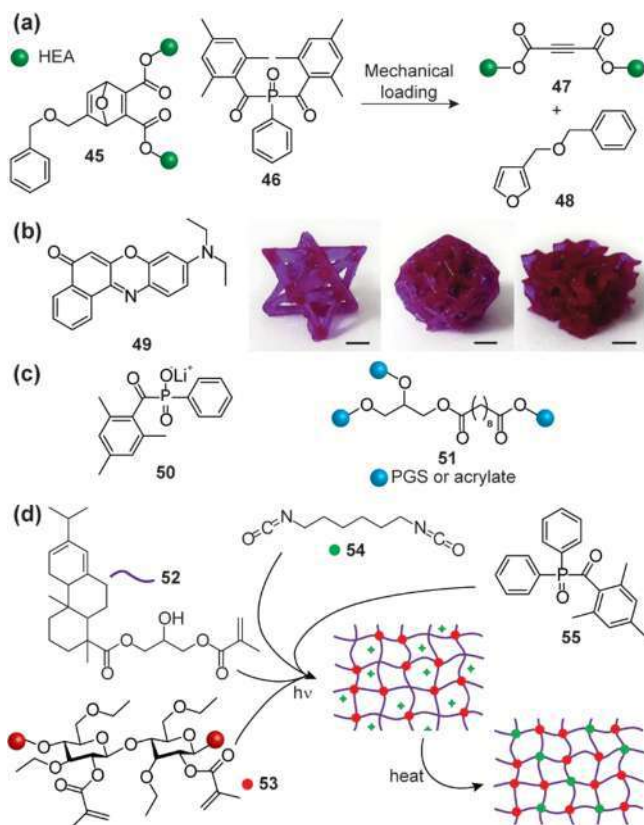


Figure 15. (a) Schematic representation of mechanical response of 45. (b) Structure of Nile red 49 and printed object containing 45 and 49. Reprinted with permission from ref 135. Copyright Elsevier. (c) Structure of LAP photoinitiators and a photo-cross-linkable 51. (d) Schematic representation of 3DP thermoset initiated by 52. Reprinted with permission from ref 138. Copyright John Wiley and Sons.

hydroxy moieties to improve the mechanical and thermal properties of the polymer (Figure 15d). The obtained sample was also characterized by self-healing by exposing the “broken moieties” to UV curing and heating, shape-memory behavior, and aggregation-induced emission. Moreover, the fluorescence, mainly due to the rosin, was shifted from 467 to 498 nm upon curing/heating treatment making this sample suitable to applications as sensor, organic light-emitting diodes and in biology.

All the reported examples show some interesting preliminary results obtained by merging functional materials to SLA/DLP techniques covering a large library of matrices, dyes.

The possibility to create new materials responsive to external stimuli could allow the improvement in the device performances covering biomedical, functional materials, basic science and industrial applications fields. Biomedical devices, artificial membranes, low-cost waveguides, emitting polymers, thermal, humidity, and light sensors are only a few examples of the great potentiality of this emerging technology.

**Organic Molecules and Dyes in TPP.** In TPP field, very few works report the use of dyes, due to the lower impact of such molecules to improve the printing performances. In fact, in TPP, the ultra-focalized irradiation and the multiple photons polymerization mechanisms are sufficient to ensure the micrometer or nanometer resolution of the structures.

Nevertheless, azodyes as 56–58 have been employed to evaluate the trans/cis photoisomerization and their applic-

ability in TPP (Figure 16a).<sup>139</sup> Alkyl and bulky groups were introduced on the dyes’ scaffolds to improve the solubility and

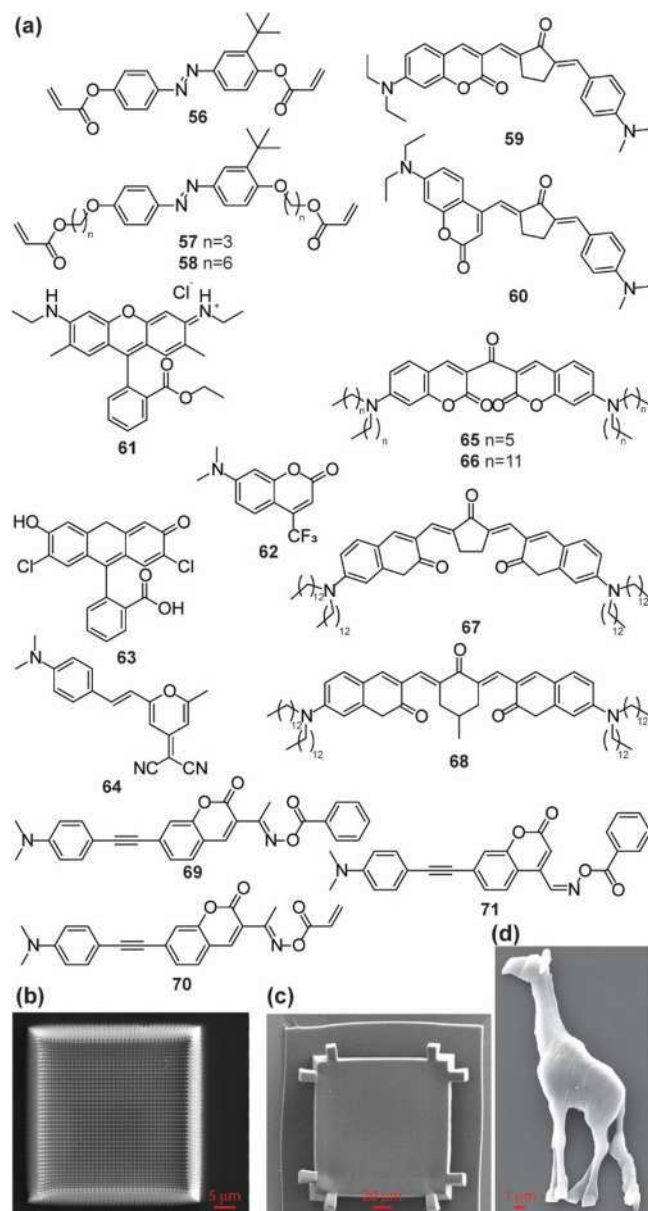


Figure 16. (a) Structures of dyes used in TPP. (b) SEM image of photonic crystal with 58. Reprinted with permission from ref 139. Copyright John Wiley and Sons. (c) SEM image of 35 containing printed a micromembrane. Reprinted from ref 140 with permission from The Royal Society of Chemistry. (d) Fabricated giraffe obtained with 60 and 61. Reprinted with permission from ref 141. Copyright 2010 American Chemical Society.

the dispersion while avoiding the formation of hydrogel with consequent dyes aggregation while printing photonic crystals (Figure 16b).

A similar azobenzene dye 35 was embedded in a polymeric matrix using BEDA 2EO as a crosslinking monomer, 46 as a photoinitiator in a 1:97:2 ratio to obtain a rapid yet reversible deformation of printed nanometer membranes (Figure 16c).<sup>140</sup> The formulation was printed to form a square membrane of 120 μm dimension which, under 532 nm laser irradiation, has shown a volume expansion of 28% and a decrease in the refractive index of about 0.16. The reversibility

of the process was demonstrated by observing the deformation and recovery by switching on and off the laser several times. Nevertheless, the weakness of the system was related to the possible photobleaching of the azodye because of the energetic laser irradiation.

Also coumarins **59** and **60** have found applications in TPP, to reduce the amount of photoinitiator needed to start the polymerization, as well as of the sub-products residue left at the end of the polymerization.<sup>141</sup> Novel coumarin derivatives were prepared with substituent groups to expand the conjugation, covering the visible spectra, to enhance the photosensitizer effect with a concurrent reduction of the photoinitiator concentration from 1-2% to 0.4%. At the same time, a good printing resolution was achieved, as demonstrated by the 3DP giraffe (Figure 16d). Coumarins and other commercial dyes **61–64**, as fluorescein, were also used to create 3DP objects able to emit light without reducing the printing resolution and enabling the internal structure verification by optical microscopy.<sup>142</sup> Coumarin-based ketones **65–68** were instead used as initiators in TPP, evaluating their photochemical and photophysical properties by varying the side chains as well as the central ketone ring.<sup>143</sup> Similarly coumarins **69–71** bearing oxime-esters groups were able to start the polymerization process upon irradiation in the 400–460 nm spectral window with low-intensity laser.<sup>62</sup>

## CONCLUSION AND PERSPECTIVES

In 3DP field, dyes have conventional uses mainly for aesthetical purposes (i.e. desired colors) or, in the best case, as elements to enhance the resolution of the printed structures. In this Review, we have reported recent advances on the use of dyes for imparting functional properties to materials: dyes can confer specific properties such as modification of mechanical behavior, light emission, tunable permeability, controlled wettability or mechanochromic features. Furthermore, these investigations can spread all over the most common 3DP technologies by adapting the chromophores' functionalization to the particular technique.

Functional devices, such as waveguides, sensors for humidity and solvents, biosubstrates, and artificial membranes can be produced. Future applications can be based on inclusion of other responsive dyes, such as derivatives of pyrene or benzoxadiazole to evaluate changes in pH, temperature or the hydrophilic/hydrophobic behavior of the polymeric matrices.<sup>8</sup> BODIPY, porphyrin, rhodamine, and carbazole can find applications in temperature sensing by the changes of the emission properties and quantum yield.<sup>5</sup> The resulting devices can be used as reversible sensors and potential biomedical drug delivery systems and actuators.<sup>144,145</sup> In particular, for biomedical applications, the biocompatibility of dyes, as well as of the degradation by-products must be considered. This should be translated in finding an appropriate compromise between the desired photophysical features of the materials and the short- and long-term cytotoxicity of the chromophores, photoinitiators, and the related degradation products.<sup>146,147</sup> A well-defined dyes functionalization with biocompatible moieties, that can promote and facilitate the biodegradation, or tuning the dyes features in the near infrared range could enhance the use in biomedical field.<sup>148</sup>

Despite the remarkable results achieved in the latest years in 3DP with various functional or staining dyes, few challenges still require to be addressed to improve the overall process and the properties of the printed objects. First of all, to expand the

use of dyes in FFF and SLS technologies, it is necessary to develop dyes with improved thermal stability. Moreover, one of the key limitations in the use of dyes in 3DP is related to their solubility into the formulations or polymeric matrices. The precipitation or aggregation of chromophores during the printing process can lead to dishomogeneities that may affect the mechanical and functional properties in the final objects. To overcome this limitation, solvents, able to evaporate during the printing process, can be added in the formulation. Nevertheless, the amount of solvents must be limited to avoid uneven evaporation during the printing process, excessive drop of the formulation viscosity and homogeneity, side effect on the polymerization. Another option consists in modifying the structure of the dyes adding side chains that can improve the compatibility with the formulation or polymeric matrix. It is worth mentioning that synthetic approaches to tune the photophysical properties and to improve the solubility of dyes and photoinitiators, by decorating the molecular scaffold with various functionalities, are nowadays of interest both in academia and industry.

The innovations presented here demonstrates that this area is still growing, and this will enlarge the applications of 3D printing. The wide variety of possible functionalities provided by dyes to common polymeric matrices will prompt both academic and industrial researchers to expand even more the progress in this field.

## AUTHOR INFORMATION

### Corresponding Authors

**Andrea Fin** – Department of Drug Science and Technology, University of Turin, Turin 10125, Italy; [orcid.org/0000-0002-7567-4646](https://orcid.org/0000-0002-7567-4646); Email: [andrea.fin@unito.it](mailto:andrea.fin@unito.it)

**Ignazio Roppolo** – Department of Applied Science and Technology DISAT, Politecnico di Torino, Turin 10129, Italy; [orcid.org/0000-0001-7602-4015](https://orcid.org/0000-0001-7602-4015); Email: [ignazio.roppolo@polito.it](mailto:ignazio.roppolo@polito.it)

### Authors

**Matteo Gastaldi** – Department of Chemistry and NIS Interdepartmental Centre and INSTM Reference Centre, University of Turin, Turin 10125, Italy

**Francesca Cardano** – Department of Chemistry and NIS Interdepartmental Centre, University of Turin, Turin 10125, Italy

**Marco Zanetti** – Department of Chemistry and NIS Interdepartmental Centre, INSTM Reference Centre, and ICxT Interdepartmental Centre, University of Turin, Turin 10125, Italy

**Guido Viscardi** – Department of Chemistry and NIS Interdepartmental Centre and INSTM Reference Centre, University of Turin, Turin 10125, Italy

**Claudia Barolo** – Department of Chemistry and NIS Interdepartmental Centre, INSTM Reference Centre, and ICxT Interdepartmental Centre, University of Turin, Turin 10125, Italy; [orcid.org/0000-0003-0627-2579](https://orcid.org/0000-0003-0627-2579)

**Silvia Bordiga** – Department of Chemistry and NIS Interdepartmental Centre and INSTM Reference Centre, University of Turin, Turin 10125, Italy; [orcid.org/0000-0003-2371-4156](https://orcid.org/0000-0003-2371-4156)

**Shlomo Magdassi** – Casali Center for Applied Chemistry, Institute of Chemistry, The Hebrew University of Jerusalem, Jerusalem 91904, Israel; [orcid.org/0000-0002-6794-0553](https://orcid.org/0000-0002-6794-0553)

Complete contact information is available at:  
<https://pubs.acs.org/10.1021/acsmaterialslett.0c00455>

### Author Contributions

All authors have given approval to the final version of the manuscript.

### Funding

The authors acknowledge the funding support by SMART3D project, financed by MIUR and Piedmont Region agreement in the framework of "Smart Industry"

### Notes

The authors declare no competing financial interest.

## REFERENCES

- (1) Pucci, A.; Ruggeri, G. Mechanochromic polymer blends. *J. Mater. Chem.* **2011**, *21*, 8282–8291.
- (2) Barber, R. W.; McFadden, M. E.; Hu, X.; Robb, M. J. Mechanochromically Gated Photoswitching: Expanding the Scope of Polymer Mechanochromism. *Synlett* **2019**, *30*, 1725–1732.
- (3) Breul, A. M.; Hager, M. D.; Schubert, U. S. Fluorescent Monomers as Building Blocks for Dye Labeled Polymers: Synthesis and Application in Energy Conversion, Biolabeling and Sensors. *Chem. Soc. Rev.* **2013**, *42*, 5366–5407.
- (4) Kubo, Y.; Nishiyabu, R. White-Light Emissive Materials Based on Dynamic Polymerization in Supramolecular Chemistry. *Polymer* **2017**, *128*, 257–275.
- (5) Pietsch, C.; Schubert, U. S.; Hoogenboom, R. Aqueous Polymeric Sensors Based on Temperature-Induced Polymer Phase Transitions and Solvatochromic. *Chem. Commun.* **2011**, *47*, 8750–8765.
- (6) Roberts, D. R. T.; Holder, S. J. Mechanochromic Systems for the Detection of Stress, Strain and Deformation in Polymeric Materials. *J. Mater. Chem.* **2011**, *21*, 8256–8268.
- (7) Kim, J.-H.; Jung, Y.; Lee, D.; Jang, W.-D. Thermoresponsive Polymer and Fluorescent Dye Hybrids for Tunable Multicolor Emission. *Adv. Mater.* **2016**, *28*, 3499–3503.
- (8) Hu, J.; Liu, S. Responsive Polymers for Detection and Sensing Applications: Current Status and Future Developments. *Macromolecules* **2010**, *43*, 8315–8330.
- (9) Jochum, F. D.; Theato, P. Temperature- and Light-Responsive Smart Polymer Materials. *Chem. Soc. Rev.* **2013**, *42*, 7468–7483.
- (10) Kocak, G.; Tuncer, C.; Büttin, V. pH-Responsive Polymers. *Polym. Chem.* **2017**, *8*, 144–176.
- (11) Ngo, T. D.; Kashani, A.; Imbalzano, G.; Nguyen, K. T. Q.; Hui, D. Additive Manufacturing (3D Printing): A Review of Materials, Methods, Applications and Challenges. *Composites, Part B* **2018**, *143*, 172–196.
- (12) Layani, M.; Wang, X.; Magdassi, S. Novel Materials for 3D Printing by Photopolymerization. *Adv. Mater.* **2018**, *30*, 1706344.
- (13) Vaezi, M.; Seitz, H.; Yang, S. A Review on 3D Micro-Additive Manufacturing Technologies. *Int. J. Adv. Manuf. Technol.* **2013**, *67*, 1721–1754.
- (14) Fantino, E.; Chiappone, A.; Roppolo, I.; Manfredi, D.; Bongiovanni, R.; Pirri, C. F.; Calignano, F. 3D Printing of Conductive Complex Structures with In Situ Generation of Silver Nanoparticles. *Adv. Mater.* **2016**, *28*, 3712–3717.
- (15) Vitale, A.; Cabral, J. T. Frontal Conversion and Uniformity in 3D Printing by Photopolymerisation. *Materials* **2016**, *9*, 760.
- (16) Han, P. Additive Design and Manufacturing of Jet Engine Parts. *Engineering* **2017**, *3*, 648–652.
- (17) Tepylo, N.; Huang, X.; Patnaik, P. C. Laser-Based Additive Manufacturing Technologies for Aerospace Applications. *Adv. Eng. Mater.* **2019**, *21*, 1900617.
- (18) Xu, Y.; Wu, X.; Guo, X.; Kong, B.; Zhang, M.; Qian, X.; Mi, S.; Sun, W. The Boom in 3D-Printed Sensor Technology. *Sensors* **2017**, *17*, 1166.
- (19) Gladman, A. S.; Garcia-Leiner, M.; Sauer-Budge, A. F. Emerging Polymeric Materials in Additive Manufacturing for Use in Biomedical Applications. *AIMS Bioeng.* **2019**, *6*, 1.
- (20) Ratheesh, G.; Venugopal, J. R.; Chinappan, A.; Ezhilarasu, H.; Sadiq, A.; Ramakrishna, S. 3D Fabrication of Polymeric Scaffolds for Regenerative Therapy. *ACS Biomater. Sci. Eng.* **2017**, *3*, 1175–1194.
- (21) Bhargav, A.; Sanjairaj, V.; Rosa, V.; Feng, L. W.; Fuh YH, J. Applications of Additive Manufacturing in Dentistry: A Review. *J. Biomed. Mater. Res., Part B* **2018**, *106*, 2058–2064.
- (22) Hull, C. W.; Gabriel, S. Apparatus for Production of Three-Dimensional Objects by Stereolithography U.S. Patent 4575330, March 11, 1986.
- (23) Crump, S. S.; Muir, A. E.-P. D. Apparatus and Method for Creating Three-Dimensional Objects U.S. Patent 5121329, June 9, 1992.
- (24) Deckard, C. R.; Darrah, J. F. Methods for Selective Laser Sintering with Layerwise Cross-Scanning U.S. Patent 5155324, October 13, 1992.
- (25) Stansbury, J. W.; Idacavage, M. J. 3D Printing with Polymers: Challenges among Expanding Options and Opportunities. *Dent. Mater.* **2016**, *32*, 54–64.
- (26) Shin, I.; Park, M. 3D Printed Conductive Patterns Based on Laser Irradiation. *Phys. Status Solidi A* **2017**, *214*, 1600943.
- (27) Anant Pidge, P.; Kumar, H. Additive Manufacturing: A Review on 3D Printing of Metals and Study of Residual Stress, Buckling Load Capacity of Strut Members. *Mater. Today Proc.* **2020**, *21*, 1689–1694.
- (28) Krakhmatova, V. Yu.; Zakharov, A. I.; Andreev, D. V.; Krivoshchepov, A. F. Methods of Additive Technologies for the Manufacture of Ceramic Products. *Glass Ceram.* **2019**, *75*, 479–484.
- (29) McCormack, A.; Highley, C. B.; Leslie, N. R.; Melchels, F. P. W. 3D Printing in Suspension Baths: Keeping the Promises of Bioprinting Afloat. *Trends Biotechnol.* **2020**, *38*, 584–593.
- (30) Mu, X.; Fitzpatrick, V.; Kaplan, D. L. From Silk Spinning to 3D Printing: Polymer Manufacturing Using Directed Hierarchical Molecular Assembly. *Adv. Healthcare Mater.* **2020**, *9*, 1901552.
- (31) Frketic, J.; Dickens, T.; Ramakrishnan, S. Automated Manufacturing and Processing of Fiber-Reinforced Polymer (FRP) Composites: An Additive Review of Contemporary and Modern Techniques for Advanced Materials Manufacturing. *Addit. Manuf.* **2017**, *14*, 69–86.
- (32) Daminabo, S. C.; Goel, S.; Grammatikos, S. A.; Nezhad, H. Y.; Thakur, V. K. Fused Deposition Modeling-Based Additive Manufacturing (3D Printing): Techniques for Polymer Material Systems. *Mater. Today Chem.* **2020**, *16*, 100248.
- (33) Zhou, P.; Qi, H.; Zhu, Z.; Qin, H.; Li, H.; Chu, C.; Yan, M. Development of SiC/PVB Composite Powders for Selective Laser Sintering Additive Manufacturing of SiC. *Materials* **2018**, *11*, 2012.
- (34) Li, L.; Lin, Q.; Tang, M.; Duncan, A. J. E.; Ke, C. Advanced Polymer Designs for Direct-Ink-Write 3D Printing. *Chem. - Eur. J.* **2019**, *25*, 10768–10781.
- (35) Long, T. E.; Williams, C. B.; Bortner, M. J. Introduction for Polymer Special Issue: Advanced Polymers for 3D Printing/Additive Manufacturing. *Polymer* **2018**, *152*, 2–3.
- (36) Pekkanen, A. M.; Mondschein, R. J.; Williams, C. B.; Long, T. E. 3D Printing Polymers with Supramolecular Functionality for Biological Applications. *Biomacromolecules* **2017**, *18*, 2669–2687.
- (37) Ligon, S. C.; Liska, R.; Stampfl, J.; Gurr, M.; Mühlaupt, R. Polymers for 3D Printing and Customized Additive Manufacturing. *Chem. Rev.* **2017**, *117*, 10212–10290.
- (38) Zhao, H.; Liu, X.; Zhao, W.; Wang, G.; Liu, B. An Overview of Research on FDM 3D Printing Process of Continuous Fiber Reinforced Composites. *J. Phys.: Conf. Ser.* **2019**, *1213*, 052037.
- (39) Mohamed, O. A.; Masood, S. H.; Bhowmik, J. L. Optimization of Fused Deposition Modeling Process Parameters: A Review of Current Research and Future Prospects. *Adv. Manuf.* **2015**, *3*, 42–53.
- (40) Brenken, B.; Barocio, E.; Favaloro, A.; Kunc, V.; Pipes, R. B. Fused Filament Fabrication of Fiber-Reinforced Polymers: A Review. *Addit. Manuf.* **2018**, *21*, 1–16.

- (41) Tan, H. W.; An, J.; Chua, C. K.; Tran, T. Metallic Nanoparticle Inks for 3D Printing of Electronics. *Adv. Electron. Mater.* **2019**, *5*, 1800831.
- (42) Gross, B. C.; Erkal, J. L.; Lockwood, S. Y.; Chen, C.; Spence, D. M. Evaluation of 3D Printing and Its Potential Impact on Biotechnology and the Chemical Sciences. *Anal. Chem.* **2014**, *86*, 3240–3253.
- (43) Singh, M.; Jonnalagadda, S. Advances in Bioprinting Using Additive Manufacturing. *Eur. J. Pharm. Sci.* **2020**, *143*, 105167.
- (44) Schmid, M.; Amado, A.; Wegener, K. Materials Perspective of Polymers for Additive Manufacturing with Selective Laser Sintering. *J. Mater. Res.* **2014**, *29*, 1824–1832.
- (45) Wendel, B.; Rietzel, D.; Kühnlein, F.; Feulner, R.; Hülde, G.; Schmachtenberg, E. Additive Processing of Polymers. *Macromol. Mater. Eng.* **2008**, *293*, 799–809.
- (46) Shafraneck, R. T.; Millik, S. C.; Smith, P. T.; Lee, C.-U.; Boydston, A. J.; Nelson, A. Stimuli-Responsive Materials in Additive Manufacturing. *Prog. Polym. Sci.* **2019**, *93*, 36–67.
- (47) Ghilan, A.; Chiriac, A. P.; Nita, L. E.; Rusu, A. G.; Neamtu, I.; Chiriac, V. M. Trends in 3D Printing Processes for Biomedical Field: Opportunities and Challenges. *J. Polym. Environ.* **2020**, *28*, 1345–1367.
- (48) Chia, H. N.; Wu, B. M. Recent Advances in 3D Printing of Biomaterials. *J. Biol. Eng.* **2015**, *9*, 4.
- (49) Lewis, J. A. Direct Ink Writing of 3D Functional Materials. *Adv. Funct. Mater.* **2006**, *16*, 2193–2204.
- (50) Aydogdu, M. O.; Mutlu, B.; Kurt, M.; Inan, A. T.; Kuruca, S. E.; Erdemir, G.; Sahin, Y. M.; Ekren, N.; Oktar, F. N.; Gunduz, O. Developments of 3D Polycaprolactone/Beta-Tricalcium Phosphate/Collagen Scaffolds for Hard Tissue Engineering. *J. Aust. Ceram. Soc.* **2019**, *55*, 849–855.
- (51) Ji, Z.; Jiang, D.; Zhang, X.; Guo, Y.; Wang, X. Facile Photo and Thermal Two-Stage Curing for High-Performance 3D Printing of Poly(Dimethylsiloxane). *Macromol. Rapid Commun.* **2020**, *41*, 2000064.
- (52) Skylar-Scott, M. A.; Mueller, J.; Visser, C. W.; Lewis, J. A. Voxellated Soft Matter via Multimaterial Multinozzle 3D Printing. *Nature* **2019**, *575*, 330–335.
- (53) Guo, Y.; Xu, J.; Yan, C.; Chen, Y.; Zhang, X.; Jia, X.; Liu, Y.; Wang, X.; Zhou, F. Direct Ink Writing of High Performance Architected Polyimides with Low Dimensional Shrinkage. *Adv. Eng. Mater.* **2019**, *21*, 1801314.
- (54) Mohan, T.; Dobaj Štiglic, A.; Beaumont, M.; Konnerth, J.; Gürer, F.; Makuc, D.; Maver, U.; Gradišnik, L.; Plavec, J.; Kargl, R.; Stana Kleinschek, K. Generic Method for Designing Self-Standing and Dual Porous 3D Bioscaffolds from Cellulosic Nanomaterials for Tissue Engineering Applications. *ACS Appl. Bio Mater.* **2020**, *3*, 1197–1209.
- (55) Quan, H.; Zhang, T.; Xu, H.; Luo, S.; Nie, J.; Zhu, X. Photocuring 3D Printing Technique and Its Challenges. *Bioact. Mater.* **2020**, *5*, 110–115.
- (56) Garra, P.; Fouassier, J. P.; Lakhdar, S.; Yagci, Y.; Lalevé, J. Visible Light Photoinitiating Systems by Charge Transfer Complexes: Photochemistry without Dyes. *Prog. Polym. Sci.* **2020**, *107*, 101277.
- (57) Shao, J.; Huang, Y.; Fan, Q. Visible Light Initiating Systems for Photopolymerization: Status, Development and Challenges. *Polym. Chem.* **2014**, *5*, 4195–4210.
- (58) Zhu, J.; Zhang, Q.; Yang, T.; Liu, Y.; Liu, R. 3D Printing of Multi-Scalable Structures via High Penetration near-Infrared Photopolymerization. *Nat. Commun.* **2020**, *11*, 3462.
- (59) Strehmel, B.; Schmitz, C.; Bromme, T.; Halbhüner, A.; Oprych, D.; Gutmann, J. S. Advances of Near Infrared Sensitized Radical and Cationic Photopolymerization: From Graphic Industry to Traditional Coatings. *J. Photopolym. Sci. Technol.* **2016**, *29*, 111–121.
- (60) Barner-Kowollik, C.; Bastmeyer, M.; Blasco, E.; Delaittre, G.; Müller, P.; Richter, B.; Wegener, M. 3D Laser Micro- and Nanoprinting: Challenges for Chemistry. *Angew. Chem., Int. Ed.* **2017**, *56*, 15828–15845.
- (61) Fourkas, J. T. Chapter 1.3—Fundamentals of Two-Photon Fabrication. In *Three-Dimensional Microfabrication Using Two-Photon Polymerization*, 2nd ed.; Baldacchini, T., Ed.; Micro and Nano Technologies; William Andrew Publishing, 2020; pp 57–76.
- (62) Qiu, W.; Hu, P.; Zhu, J.; Liu, R.; Li, Z.; Hu, Z.; Chen, Q.; Dietliker, K.; Liska, R. Cleavable Unimolecular Photoinitiators Based on Oxime-Ester Chemistry for Two-Photon Three-Dimensional Printing. *ChemPhotoChem.* **2019**, *3*, 1090–1094.
- (63) Wang, J.; Goyanes, A.; Gaisford, S.; Basit, A. W. Stereolithographic (SLA) 3D Printing of Oral Modified-Release Dosage Forms. *Int. J. Pharm.* **2016**, *503*, 207–212.
- (64) Kim, L. U.; Kim, J. W.; Kim, C. K. Effects of Molecular Structure of the Resins on the Volumetric Shrinkage and the Mechanical Strength of Dental Restorative Composites. *Biomacromolecules* **2006**, *7*, 2680–2687.
- (65) Moraes, R. R.; Garcia, J. W.; Barros, M. D.; Lewis, S. H.; Pfeifer, C. S.; Liu, J.; Stansbury, J. W. Control of Polymerization Shrinkage and Stress in Nanogel-Modified Monomer and Composite Materials. *Dent. Mater.* **2011**, *27*, 509–519.
- (66) Kloxin, C. J.; Scott, T. F.; Bowman, C. N. Stress Relaxation via Addition-Fragmentation Chain Transfer in a Thiol-Ene Photopolymerization. *Macromolecules* **2009**, *42*, 2551–2556.
- (67) Lu, H.; Carioscia, J. A.; Stansbury, J. W.; Bowman, C. N. Investigations of Step-Growth Thiol-Ene Polymerizations for Novel Dental Restoratives. *Dent. Mater.* **2005**, *21*, 1129–1136.
- (68) Lee, T. Y.; Carioscia, J.; Smith, Z.; Bowman, C. N. Thiol-Allyl Ether-Methacrylate Ternary Systems. Evolution Mechanism of Polymerization-Induced Shrinkage Stress and Mechanical Properties. *Macromolecules* **2007**, *40*, 1473–1479.
- (69) Park, H. Y.; Kloxin, C. J.; Scott, T. F.; Bowman, C. N. Stress Relaxation by Addition-Fragmentation Chain Transfer in Highly Cross-Linked Thiol-Yne Networks. *Macromolecules* **2010**, *43*, 10188–10190.
- (70) Hu, P.; Qiu, W.; Naumov, S.; Scherzer, T.; Hu, Z.; Chen, Q.; Knolle, W.; Li, Z. Conjugated Bifunctional Carbazole-Based Oxime Esters: Efficient and Versatile Photoinitiators for 3D Printing under One- and Two-Photon Excitation. *ChemPhotoChem.* **2020**, *4*, 224–232.
- (71) Zhang, X.; Jiang, X. N.; Sun, C. Micro-Stereolithography of Polymeric and Ceramic Microstructures. *Sens. Actuators, A* **1999**, *77*, 149–156.
- (72) Wang, F.; Chong, Y.; Wang, F.; He, C. Photopolymer Resins for Luminescent Three-Dimensional Printing. *J. Appl. Polym. Sci.* **2017**, *134*, 44988.
- (73) Chen, H.; Noirbent, G.; Sun, K.; Brunel, D.; Gignes, D.; Morlet-Savary, F.; Zhang, Y.; Liu, S.; Xiao, P.; Dumur, F.; Lalevé, J. Photoinitiators Derived from Natural Product Scaffolds: Mono-chalcones in Three-Component Photoinitiating Systems and Their Applications in 3D Printing. *Polym. Chem.* **2020**, *11*, 4647–4659.
- (74) Kulinich, A. V.; Ishchenko, A. A. Structures and Fluorescence Spectra of Merocyanine Dyes in Polymer Films. *J. Appl. Spectrosc.* **2019**, *86*, 35–42.
- (75) Hu, S.; Zou, J.; Zhou, G.; Li, D.; Wu, H.; Su, S.; Wong, W.-Y.; Yang, W.; Peng, J.; Cao, Y. Highly Efficient Pure White Polymer Light-Emitting Devices Based on Poly(N-Vinylcarbazole) Doped with Blue and Red Phosphorescent Dyes. *Sci. China: Chem.* **2011**, *54*, 671–677.
- (76) Gašiorski, P.; Matusiewicz, M.; Gondek, E.; Pokladko-Kowar, M.; Armatys, P.; Wojtasik, K.; Danel, A.; Uchacz, T.; Kityk, A. V. Efficient Green Electroluminescence from 1,3-Diphenyl-1H-Pyrazolo-[3,4-b]Quinoxaline Dyes in Dye-Doped Polymer Based Electro-luminescent Devices. *Dyes Pigm.* **2018**, *151*, 380–384.
- (77) Bustamante, N.; Ielasi, G.; Bedoya, M.; Orellana, G. Optimization of Temperature Sensing with Polymer-Embedded Luminescent Ru(II) Complexes. *Polymers* **2018**, *10*, 234.
- (78) Ciardelli, F.; Ruggeri, G.; Pucci, A. Dye-Containing Polymers: Methods for Preparation of Mechanochromic Materials. *Chem. Soc. Rev.* **2013**, *42*, 857–870.

- (79) Kumar, P.; Sharma, V.; Raina, K. K. Studies on Inter-Dependency of Electrooptic Characteristics of Orange Azo and Blue Anthraquinone Dichroic Dye Doped Polymer Dispersed Liquid Crystals. *J. Mol. Liq.* **2018**, *251*, 407–416.
- (80) Roppolo, I.; Chiappone, A.; Angelini, A.; Stassi, S.; Frascella, F.; Pirri, C. F.; Ricciardi, C.; Descrovi, E. 3D Printable Light-Responsive Polymers. *Mater. Horiz.* **2017**, *4*, 396–401.
- (81) Cheng, Q.; Zheng, Y.; Wang, T.; Sun, D.; Lin, R. Yellow Resistant Photosensitive Resin for Digital Light Processing 3D Printing. *J. Appl. Polym. Sci.* **2020**, *137*, 48369.
- (82) Peng, B.; Yang, Y.; Gu, K.; Amis, E. J.; Cavicchi, K. A. Digital Light Processing 3D Printing of Triple Shape Memory Polymer for Sequential Shape Shifting. *ACS Materials Lett.* **2019**, *1*, 410–417.
- (83) Lee, M. P.; Cooper, G. J. T.; Hinkley, T.; Gibson, G. M.; Padgett, M. J.; Cronin, L. Development of a 3D Printer Using Scanning Projection Stereolithography. *Sci. Rep.* **2015**, *5*, 9875.
- (84) Theato, P.; Sumerlin, B. S.; O'Reilly, R. K.; Epps, T. H., III Stimuli Responsive Materials. *Chem. Soc. Rev.* **2013**, *42*, 7055–7056.
- (85) Maldonado, N.; Vegas, V. G.; Halevi, O.; Martínez, J. I.; Lee, P. S.; Magdassi, S.; Wharmby, M. T.; Platero-Prats, A. E.; Moreno, C.; Zamora, F.; Amo-Ochoa, P. 3D Printing of a Thermo- and Solvatochromic Composite Material Based on a Cu(II)-Thymine Coordination Polymer with Moisture Sensing Capabilities. *Adv. Funct. Mater.* **2019**, *29*, 1808424.
- (86) Li, Y.; Feng, Z.; Huang, L.; Essa, K.; Bilotti, E.; Zhang, H.; Peijs, T.; Hao, L. Additive Manufacturing High Performance Graphene-Based Composites: A Review. *Composites, Part A* **2019**, *124*, 105483.
- (87) Milazzo, M.; Contessi Negrini, N.; Scialla, S.; Marelli, B.; Farè, S.; Danti, S.; Buehler, M. J. Additive Manufacturing Approaches for Hydroxyapatite-Reinforced Composites. *Adv. Funct. Mater.* **2019**, *29*, 1903055.
- (88) Blok, L. G.; Longana, M. L.; Yu, H.; Woods, B. K. S. An Investigation into 3D Printing of Fibre Reinforced Thermoplastic Composites. *Addit. Manuf.* **2018**, *22*, 176–186.
- (89) Chang, V. Y.; Fedele, C.; Priimagi, A.; Shishido, A.; Barrett, C. J. Photoreversible Soft Azo Dye Materials: Toward Optical Control of Bio-Interfaces. *Adv. Opt. Mater.* **2019**, *7*, 1900091.
- (90) Fleischmann, C.; Lievenbrück, M.; Ritter, H. Polymers and Dyes: Developments and Applications. *Polymers* **2015**, *7*, 717–746.
- (91) Weis, P.; Tian, W.; Wu, S. Photoinduced Liquefaction of Azobenzene-Containing Polymers. *Chem. - Eur. J.* **2018**, *24*, 6494–6505.
- (92) Berkovic, G.; Krongauz, V.; Weiss, V. Spiropyran and Spirooxazines for Memories and Switches. *Chem. Rev.* **2000**, *100*, 1741–1754.
- (93) Lukyanov, B. S.; Lukyanova, M. B. Spiropyran: Synthesis, Properties, and Application. *Chem. Heterocycl. Compd.* **2005**, *41*, 281–311.
- (94) Yao, X.; Li, T.; Wang, J.; Ma, X.; Tian, H. Recent Progress in Photoswitchable Supramolecular Self-Assembling Systems. *Adv. Opt. Mater.* **2016**, *4*, 1322–1349.
- (95) Trenor, S. R.; Shultz, A. R.; Love, B. J.; Long, T. E. Coumarins in Polymers: From Light Harvesting to Photo-Cross-Linkable Tissue Scaffolds. *Chem. Rev.* **2004**, *104*, 3059–3078.
- (96) Klajn, R. Spiropyran-Based Dynamic Materials. *Chem. Soc. Rev.* **2014**, *43*, 148–184.
- (97) Angiolini, L.; Benelli, T.; Giorgini, L.; Raymo, F. M. Optical and Chiroptical Switches Based on Photoinduced Photon and Proton Transfer in Copolymers Containing Spiropyran and Azopyridine Chromophores in Their Side Chains. *Polymer* **2009**, *50*, S638–S646.
- (98) Weis, P.; Wu, S. Light-Switchable Azobenzene-Containing Macromolecules: From UV to Near Infrared. *Macromol. Rapid Commun.* **2018**, *39*, 1700220.
- (99) Bushuyev, O. S.; Aizawa, M.; Shishido, A.; Barrett, C. J. Shape-Shifting Azo Dye Polymers: Towards Sunlight-Driven Molecular Devices. *Macromol. Rapid Commun.* **2018**, *39*, 1700253.
- (100) Tasiar, M.; Kim, D.; Singha, S.; Krzeszewski, M.; Ahn, K. H.; Gryko, D. T.  $\pi$ -Expanded Coumarins: Synthesis, Optical Properties and Applications. *J. Mater. Chem. C* **2015**, *3*, 1421–1446.
- (101) Liu, X.; Cole, J. M.; Waddell, P. G.; Lin, T.-C.; Radia, J.; Zeidler, A. Molecular Origins of Optoelectronic Properties in Coumarin Dyes: Toward Designer Solar Cell and Laser Applications. *J. Phys. Chem. A* **2012**, *116*, 727–737.
- (102) Musa, M.; Cooperwood, J.; Khan, M. O. A Review of Coumarin Derivatives in Pharmacotherapy of Breast Cancer. *Curr. Med. Chem.* **2008**, *15*, 2664–2679.
- (103) Bhosale, S. V.; Jani, C. H.; Langford, S. J. Chemistry of Naphthalene Diimides. *Chem. Soc. Rev.* **2008**, *37*, 331–342.
- (104) Al Kobaisi, M.; Bhosale, S. V.; Latham, K.; Raynor, A. M.; Bhosale, S. V. Functional Naphthalene Diimides: Synthesis, Properties, and Applications. *Chem. Rev.* **2016**, *116*, 11685–11796.
- (105) Gao, Z.; Hao, Y.; Zheng, M.; Chen, Y. A Fluorescent Dye with Large Stokes Shift and High Stability: Synthesis and Application to Live Cell Imaging. *RSC Adv.* **2017**, *7*, 7604–7609.
- (106) Paternò, G. M.; Barbero, N.; Galliano, S.; Barolo, C.; Lanzani, G.; Scotognella, F.; Borrelli, R. Excited State Photophysics of Squaraine Dyes for Photovoltaic Applications: An Alternative Deactivation Scenario. *J. Mater. Chem. C* **2018**, *6*, 2778–2785.
- (107) Hasegawa, Y.; Kitagawa, Y. Thermo-Sensitive Luminescence of Lanthanide Complexes, Clusters, Coordination Polymers and Metal-Organic Frameworks with Organic Photosensitizers. *J. Mater. Chem. C* **2019**, *7*, 7494–7511.
- (108) Löwe, C.; Weder, C. Oligo(p-Phenylene Vinylene) Excimers as Molecular Probes: Deformation-Induced Color Changes in Photoluminescent Polymer Blends. *Adv. Mater.* **2002**, *14*, 1625–1629.
- (109) Peterson, G. I.; Larsen, M. B.; Ganter, M. A.; Storti, D. W.; Boydston, A. J. 3D-Printed Mechanochromic Materials. *ACS Appl. Mater. Interfaces* **2015**, *7*, 577–583.
- (110) Dharmawardana, M.; Arimilli, B. S.; Luzuriaga, M. A.; Kwon, S.; Lee, H.; Appuhamillage, G. A.; McCandless, G. T.; Smaldone, R. A.; Gassensmith, J. J. The Thermo-Responsive Behavior in Molecular Crystals of Naphthalene Diimides and Their 3D Printed Thermo-chromic Composites. *CrystEngComm* **2018**, *20*, 6054–6060.
- (111) Dharmawardana, M.; Welch, R. P.; Kwon, S.; Nguyen, V. K.; McCandless, G. T.; Omary, M. A.; Gassensmith, J. J. Thermo-Mechanically Responsive Crystalline Organic Cantilever. *Chem. Commun.* **2017**, *53*, 9890–9893.
- (112) Boyle, B. M.; French, T. A.; Pearson, R. M.; McCarthy, B. G.; Miyake, G. M. Structural Color for Additive Manufacturing: 3D-Printed Photonic Crystals from Block Copolymers. *ACS Nano* **2017**, *11*, 3052–3058.
- (113) Wang, L. L.; Highley, C. B.; Yeh, Y.-C.; Galarraga, J. H.; Uman, S.; Burdick, J. A. Three-Dimensional Extrusion Bioprinting of Single- and Double-Network Hydrogels Containing Dynamic Covalent Crosslinks. *J. Biomed. Mater. Res., Part A* **2018**, *106*, 865–875.
- (114) Ren, Y.; Feng, J. Skin-Inspired Multifunctional Luminescent Hydrogel Containing Layered Rare-Earth Hydroxide with 3D Printability for Human Motion Sensing. *ACS Appl. Mater. Interfaces* **2020**, *12*, 6797–6805.
- (115) Trampe, E.; Koren, K.; Akkineni, A. R.; Senwitz, C.; Krutz, F.; Lode, A.; Gelinsky, M.; Kühl, M. Functionalized Bioink with Optical Sensor Nanoparticles for O<sub>2</sub> Imaging in 3D-Bioprinted Constructs. *Adv. Funct. Mater.* **2018**, *28*, 1804411.
- (116) Xia, Y.; Xue, B.; Qin, M.; Cao, Y.; Li, Y.; Wang, W. Printable Fluorescent Hydrogels Based on Self-Assembling Peptides. *Sci. Rep.* **2017**, *7*, 9691.
- (117) Li, Z.; Liu, P.; Ji, X.; Gong, J.; Hu, Y.; Wu, W.; Wang, X.; Peng, H.-Q.; Kwok, R. T. K.; Lam, J. W. Y.; Lu, J.; Tang, B. Z. Bioinspired Simultaneous Changes in Fluorescence Color, Brightness, and Shape of Hydrogels Enabled by AIEgens. *Adv. Mater.* **2020**, *32*, 1906493.
- (118) Lin, Q.; Li, L.; Tang, M.; Hou, X.; Ke, C. Rapid Macroscale Shape Morphing of 3D-Printed Polyrotaxane Monoliths Amplified from PH-Controlled Nanoscale Ring Motions. *J. Mater. Chem. C* **2018**, *6*, 11956–11960.

- (119) Lin, Q.; Hou, X.; Ke, C. Ring Shuttling Controls Macroscopic Motion in a Three-Dimensional Printed Polyrotaxane Monolith. *Angew. Chem., Int. Ed.* **2017**, *56*, 4452–4457.
- (120) Rohde, R. C.; Basu, A.; Okello, L. B.; Barbee, M. H.; Zhang, Y.; Velev, O. D.; Nelson, A.; Craig, S. L. Mechanochromic Composite Elastomers for Additive Manufacturing and Low Strain Mechano-phore Activation. *Polym. Chem.* **2019**, *10*, 5985–5991.
- (121) Hagaman, D. E.; Leist, S.; Zhou, J.; Ji, H.-F. Photoactivated Polymeric Bilayer Actuators Fabricated via 3D Printing. *ACS Appl. Mater. Interfaces* **2018**, *10*, 27308–27315.
- (122) Govindarajan, S. R.; Xu, Y.; Swanson, J. P.; Jain, T.; Lu, Y.; Choi, J.-W.; Joy, A. A Solvent and Initiator Free, Low-Modulus, Degradable Polyester Platform with Modular Functionality for Ambient-Temperature 3D Printing. *Macromolecules* **2016**, *49*, 2429–2437.
- (123) Fertier, L.; Koleilat, H.; Stemmelen, M.; Giani, O.; Joly-Duhamel, C.; Lapinte, V.; Robin, J. J. The use of renewable feedstock in UV-curable materials - A new age for polymers and green chemistry. *Prog. Polym. Sci.* **2013**, *38*, 932–962.
- (124) Montero de Espinosa, L. M.; Meier, M. A. R. Plant oils: The perfect renewable resource for polymer science?! *Eur. Polym. J.* **2011**, *47*, 837–852.
- (125) Kabb, C. P.; O'Bryan, C. S.; Deng, C. C.; Angelini, T. E.; Sumerlin, B. S. Photoreversible Covalent Hydrogels for Soft-Matter Additive Manufacturing. *ACS Appl. Mater. Interfaces* **2018**, *10*, 16793–16801.
- (126) Sakai, S.; Ohi, H.; Hotta, T.; Kamei, H.; Taya, M. Differentiation Potential of Human Adipose Stem Cells Bioprinted with Hyaluronic Acid/Gelatin-Based Bioink through Microextrusion and Visible Light-Initiated Crosslinking. *Biopolymers* **2018**, *109*, No. e23080.
- (127) Ambulo, C. P.; Burroughs, J. J.; Boothby, J. M.; Kim, H.; Shankar, M. R.; Ware, T. H. Four-Dimensional Printing of Liquid Crystal Elastomers. *ACS Appl. Mater. Interfaces* **2017**, *9*, 37332–37339.
- (128) Gillono, M.; Roppolo, I.; Frascella, F.; Scaltrito, L.; Pirri, C. F.; Chiappone, A. CO<sub>2</sub> Permeability Control in 3D Printed Light Responsive Structures. *Appl. Mater. Today* **2020**, *18*, 100470.
- (129) Gonzalez, G.; Chiappone, A.; Dietliker, K.; Pirri, C. F.; Roppolo, I. Fabrication and Functionalization of 3D Printed Polydimethylsiloxane-Based Microfluidic Devices Obtained through Digital Light Processing. *Adv. Mater. Technol.* **2020**, 2000374.
- (130) Xie, H.; Yang, K.-K.; Wang, Y.-Z. Photo-Cross-Linking of Anthracene as a Versatile Strategy to Design Shape Memory Polymers. *Mater. Today Proc.* **2019**, *16*, 1524–1530.
- (131) Frascella, F.; González, G.; Bosch, P.; Angelini, A.; Chiappone, A.; Sangermano, M.; Pirri, C. F.; Roppolo, I. Three-Dimensional Printed Photoluminescent Polymeric Waveguides. *ACS Appl. Mater. Interfaces* **2018**, *10*, 39319–39326.
- (132) Roppolo, I.; Frascella, F.; Gastaldi, M.; Castellino, M.; Ciubini, B.; Barolo, C.; Scaltrito, L.; Nicosia, C.; Zanetti, M.; Chiappone, A. Thiol-Yne Chemistry for 3D Printing: Exploiting off Stoichiometric Route for Selective Functionalization of 3D Objects. *Polym. Chem.* **2019**, *10*, 5950–5958.
- (133) Petersen, S. R.; Wilson, J. A.; Becker, M. L. Versatile Ring-Opening Copolymerization and Postprinting Functionalization of Lactone and Poly(Propylene Fumarate) Block Copolymers: Resorbable Building Blocks for Additive Manufacturing. *Macromolecules* **2018**, *51*, 6202–6208.
- (134) Wilson, J. A.; Luong, D.; Kleinfehn, A. P.; Sallam, S.; Wesdemiotis, C.; Becker, M. L. Magnesium Catalyzed Polymerization of End Functionalized Poly(Propylene Maleate) and Poly(Propylene Fumarate) for 3D Printing of Bioactive Scaffolds. *J. Am. Chem. Soc.* **2018**, *140*, 277–284.
- (135) Cao, B.; Boechler, N.; Boydston, A. J. Additive Manufacturing with a Flex Activated Mechano-phore for Nondestructive Assessment of Mechanochemical Reactivity in Complex Object Geometries. *Polymer* **2018**, *152*, 4–8.
- (136) Shen, Y.; Tang, H.; Huang, X.; Hang, R.; Zhang, X.; Wang, Y.; Yao, X. DLP Printing Photocurable Chitosan to Build Bio-Constructs for Tissue Engineering. *Carbohydr. Polym.* **2020**, *235*, 115970.
- (137) Wang, P.; Berry, D. B.; Song, Z.; Kiratitanaporn, W.; Schimelman, J.; Moran, A.; He, F.; Xi, B.; Cai, S.; Chen, S. 3D Printing of a Biocompatible Double Network Elastomer with Digital Control of Mechanical Properties. *Adv. Funct. Mater.* **2020**, *30*, 1910391.
- (138) Lu, C.; Wang, C.; Yu, J.; Wang, J.; Chu, F. Two-Step 3 D-Printing Approach toward Sustainable, Repairable, Fluorescent Shape-Memory Thermosets Derived from Cellulose and Rosin. *ChemSusChem* **2020**, *13*, 893–902.
- (139) Wang, H.; Jin, F.; Chen, S.; Dong, X.-Z.; Zhang, Y.-L.; Chen, W.-Q.; Zhao, Z.-S.; Duan, X.-M. Preparation, Photoisomerization, and Microfabrication with Two-Photon Polymerization of Crosslinked Azo-Polymers. *J. Appl. Polym. Sci.* **2013**, *130*, 2947–2956.
- (140) Descrovi, E.; Pirani, F.; Rajamanickam, V. P.; Licheri, S.; Liberale, C. Photo-Responsive Suspended Micro-Membranes. *J. Mater. Chem. C* **2018**, *6*, 10428–10434.
- (141) Xue, J.; Zhao, Y.; Wu, F.; Fang, D.-C. Effect of Bridging Position on the Two-Photon Polymerization Initiating Efficiencies of Novel Coumarin/Benzylidene Cyclopentanone Dyes. *J. Phys. Chem. A* **2010**, *114*, 5171–5179.
- (142) Žukauskas, A.; Malinauskas, M.; Kontenis, L.; Purlys, V.; Paipulas, D.; Vengris, M.; Gadonas, R. Organic Dye Doped Microstructures for Optically Active Functional Devices Fabricated via Two-Photon Polymerization Technique. *Lith. J. Phys.* **2010**, *50*, 55–61.
- (143) Nazir, R.; Danilevicius, P.; Ciuciu, A. I.; Chatzinikolaidou, M.; Gray, D.; Flamigni, L.; Farsari, M.; Gryko, D. T.  $\pi$ -Expanded Ketocoumarins as Efficient, Biocompatible Initiators for Two-Photon-Induced Polymerization. *Chem. Mater.* **2014**, *26*, 3175–3184.
- (144) Wei, M.; Gao, Y.; Li, X.; Serpe, M. J. Stimuli-Responsive Polymers and Their Applications. *Polym. Chem.* **2017**, *8*, 127–143.
- (145) Gil, E. S.; Hudson, S. M. Stimuli-Responsive Polymers and Their Bioconjugates. *Prog. Polym. Sci.* **2004**, *29*, 1173–1222.
- (146) Melchels, F. P. W.; Feijen, J.; Grijpma, D. W. A Review on Stereolithography and Its Applications in Biomedical Engineering. *Biomaterials* **2010**, *31*, 6121–6130.
- (147) Heller, C.; Schwentenwein, M.; Russmueller, G.; Varga, F.; Stampfl, J.; Liska, R. Vinyl Esters: Low Cytotoxicity Monomers for the Fabrication of Biocompatible 3D Scaffolds by Lithography Based Additive Manufacturing. *J. Polym. Sci., Part A: Polym. Chem.* **2009**, *47*, 6941–6954.
- (148) Chen, S.; Sun, B.; Miao, H.; Wang, G.; Sun, P.; Li, J.; Wang, W.; Fan, Q.; Huang, W. NIR-II Dye-Based Multifunctional Telechelic Glycopolymers for NIR-IIa Fluorescence Imaging-Guided Stimuli-Responsive Chemo-Photothermal Combination Therapy. *ACS Materials Lett.* **2020**, *2*, 174–183.